Neuroradiology (2007) 49:1–22
DOI 10.1007/s00234-006-0156-2

DIAGNOSTIC NEURORADIOLOGY

Neuroradiological findings in vascular dementia

Ali Guermazi · Yves Miaux · Alex Rovira-Cañellas · Joyce Suhy · Jon Pauls · Ria Lopez · Holly Posner

Received: 16 May 2006 / Accepted: 30 August 2006 / Published online: 18 November 2006

Abstract
Introduction There are multiple diagnostic criteria for vascular dementia (VaD) that may define different populations. Utilizing the criteria of the National Institute of Neurological Disorders and Stroke and Association Internationale pour la Recherche et l'Enseignement en Neurosciences (NINDS-AIREN) has provided improved consistency in the diagnosis of VaD. The criteria include a table listing brain imaging lesions associated with VaD.
Methods The different neuroradiological aspects of the criteria are reviewed based on the imaging data from an ongoing large-scale clinical trial testing a new treatment for VaD. The NINDS-AIREN criteria were applied by a centralized imaging rater to determine eligibility for enrollment in 1,202 patients using brain CT or MRI.
Results Based on the above data set, the neuroradiological features that are associated with VaD and that can result from cerebral small-vessel disease with extensive leukoencephalopathy or lacunae (basal ganglia or frontal white matter), or may be the consequence of single strategically located infarcts or multiple infarcts in large-vessel territories, are illustrated. These features may also be the consequence of global cerebral hypoperfusion, intracerebral hemorrhage, or other mechanisms such as genetically determined arteriopathies.
Conclusion Neuroimaging confirmation of cerebrovascular disease in VaD provides information about the topography and severity of vascular lesions. Neuroimaging may also assist with the differential diagnosis of dementia associated with normal pressure hydrocephalus, chronic subdural hematoma, arteriovenous malformation or tumoral diseases.

Keywords Neuroimaging · CT · MRI · Vascular dementia · NINDS-AIREN criteria

Introduction

Vascular dementia (VaD) is the second most common cause of dementia, following Alzheimer disease [1, 2]. The National Institute of Neurological Disorders and Stroke and Association Internationale pour la Recherche et l'Enseignement en Neurosciences (NINDS-AIREN) met in 1991 and published in 1993 their diagnostic criteria of VaD which have helped to clarify the clinical and neuroimaging diagnosis for VaD [3, 4]. These criteria, which have been validated by some neuropathological studies [5–7] and a centralized imaging rater to determine eligibility for enrollment in recent large-scale clinical trials testing new treatments for VaD, have provided increased consistency in the diagnosis of VaD. Neuroimaging is required for confirmation of cerebrovascular disease in VaD and provides information about the topography and severity of the vascular lesions. Neuroimaging may also assist with the differential diagnosis of dementia associated with normal

This work was presented at the ESNR 2005 (Barcelona, Spain) and is a recipient of a Cum Laude Award.

A. Guermazi (✉) · Y. Miaux · J. Suhy · J. Pauls · R. Lopez
Department of Radiology Services, Synarc, Inc.,
575 Market Street, 17th Floor,
San Francisco, CA 94105, USA
e-mail: ali.guermazi@synarc.com

A. Rovira-Cañellas
Unita de Resonància Magnètica,
Hospital General Universitari Vall d'Hebron,
Barcelona, Spain

H. Posner
Eisai, Inc.,
Teaneck, NJ, USA

pressure hydrocephalus, chronic subdural hematoma, arteriovenous malformation or tumoral diseases.

Definition

The diagnosis of VaD requires dementia with a decline in memory and intellectual ability that causes impaired functioning in daily living, associated with evidence of cerebrovascular disease demonstrated by either history, or clinical examination, and brain imaging. A temporal association between dementia and cerebrovascular disease is mandatory for the definite diagnosis of VaD (Table 1) [8–11]. Indeed, the onset of dementia should be within 3 months following a recognized stroke. Although abrupt onset of dementia may be confused with abrupt recognition, and possibly endorsed by care-takers of patients with Alzheimer disease [12, 13], the possibility of misdiagnosis should be minimized if there is either clinical or brain imaging evidence of stroke [4, 14, 15].

Pathophysiology

The pathophysiology of VaD incorporates interactions between vascular etiologies (cerebrovascular disease and vascular risk factors), changes in the brain (infarcts, white matter lesions, atrophy), host factors (age, education, vascular risk factors) and cognition (Table 2) [1, 16–20]. Longitudinal studies have recognized the central role of recurrent stroke as a risk factor for incident dementia [21].

Animal and human studies have indicated that, as with Alzheimer disease, deficits in cholinergic transmission—including nicotinic receptor binding abnormalities—may be responsible for the development of cognitive impairment associated with VaD. Therefore, studies of acetylcholinesterase inhibitors (AChEIs) have been initiated and have shown promising results to date. These agents have demonstrated cognitive and global benefits in patients with VaD. Additionally, functional and behavioral benefits have been reported with the dual-mechanism AChEI galantamine [22–24].

Table 1 NINDS-AIREN criteria for probable VaD

Criteria	Description
1 Dementia	
2 Cerebrovascular disease defined by one of:	History of cerebrovascular disease
	Focal signs on examination (with or without history)
	CT/MRI showing lesions that confirm cerebrovascular disease
3 Temporal relationship between 1 and 2 demonstrated by one of:	Onset of dementia within 3 months following stroke
	Abrupt deterioration in cognitive functions
	Fluctuating, stepwise progression of cognitive deficits

Table 2 Risk factors for VaD

Factors	Description
1 Non-reversible risk factors	Increasing age
	Genetic predisposition (e.g. CADASIL)
	Geographic origin (e.g. African descent, Asian)
	Prior strokes (particularly if large, multiple, or in vulnerable locations)
	Low educational level
2 Reversible risk factors	Hypertension
	Coronary artery disease
	Atrial fibrillation
	Diabetes mellitus
	Hyperlipidemia
	Hyperglycemia
	Smoking

Clinical criteria

VaD is a broad term that encompasses all instances of dementia associated not only with ischemic cerebrovascular disease but also with hemorrhagic, hypoxic–ischemic cerebral lesions such as those due to cardiac arrest, and senile leukoencephalopathic lesions. It excludes patients with pure asphyxia or respiratory failure (hypoxemic anoxia) and carbon monoxide or cyanide poisoning (histotoxic anoxia) [4]. The clinical course is variable, and may be static, remitting, or progressive. VaD is associated with specific clinical findings early in the course (e.g., gait disorder, incontinence, or mood and personality changes) that support a vascular rather than a degenerative cause [4]. Cognitive impairment still is the primary symptom of VaD [22]. Men have a higher prevalence of VaD than women in most age groups [4].

Role of imaging

CT or MRI of the brain is required for the diagnosis of VaD, with MRI being more sensitive in this respect than CT [25]. Absence of vascular lesions on brain CT or MRI rules out probable VaD and represents the most important element to distinguish Alzheimer disease from VaD [26]. There are no pathognomonic brain CT or MR images of VaD. Thus, correlation with the clinical evidence is mandatory.

To be considered as evidence in favor of VaD (probable VaD), the radiological findings should fulfill minimum standards of the NINDS-AIREN criteria for both severity and topography (large vessel and small vessel) (Table 3). Possible VaD could be diagnosed by the presence of dementia with focal neurological signs in patients in whom brain imaging studies confirming definite cerebrovascular disease are missing; or in the absence of a clear temporal relationship between dementia and stroke; or in patients with subtle onset and variable course (plateau or improvement) of cognitive deficits and evidence of relevant cerebrovascular disease [4]. These radiological NINDS-AIREN criteria for VaD have suboptimal reproducibility. Use of operational criteria has shown improvement of agreement to acceptable levels, but only in experienced readers [27].

In clinical trials, neuroimaging may detect other conditions such as brain tumor, subdural hematoma, and normal pressure hydrocephalus that may be present with dementia, but are considered as exclusion criteria for VaD.

Large-vessel disease

Arterial territorial infarct

VaD is associated with evidence of relevant cerebrovascular disease including multiple large-vessel infarcts or a single strategically placed infarct. Strategic locations include angular gyrus (Fig. 1), thalamus (Fig. 2), basal forebrain, or posterior cerebral artery (PCA) or anterior cerebral artery (ACA) territories [4]. There is a predominance of left-sided infarcts, as involvement of the dominant hemisphere is one of the criteria of severity [28]. PCA infarcts can be included only when they involve the paramedian thalamus with the cortical gray matter of the temporal/occipital lobe, or the inferior medial temporal lobe. ACA infarcts must be bilateral to meet the criteria. For the middle cerebral artery (MCA), the infarcts need to involve the parietotemporal lobe (Fig. 3) or temporooccipital lobe (Fig. 4). Indeed, patients with MCA infarcts presenting with severe aphasia must be excluded since appropriate evaluation is difficult [4].

Territorial anterior circulation infarcts, mostly related to the MCA territory, can be divided into large and limited in size. Large infarcts are those covering at least two of the three MCA territories (deep, superficial anterior and superficial posterior).

Territorial posterior circulation infarcts are divided into large territorial infarcts, brain stem infarcts, and small cerebellar infarcts. Large territorial infarcts depend on the territory of the posterior inferior (PICA), anterior inferior (AICA) and superior (SCA) cerebellar arteries and their branches, and on the territory of the PCA. Brain stem infarcts may be related to large vessels stenosis or occlusion, or to small-vessel disease involving the perforators arising from the basilar artery (brain stem lacunar infarct). Small cerebellar infarcts are less than 2 cm in size, and due to involvement of small distal arteries (end-zone infarcts).

Ill-defined pontine hyperintensity on T2-weighted MR images with only minor corresponding T1-weighted hypointensity occurring after supratentorial ischemic stroke does not fulfill the criteria for brain infarct, but it relates to poor clinical outcome. The most probable causes of this pontine hyperintensity are pontine ischemic rarefaction and Wallerian degeneration of the pyramidal tract. The pathological

Table 3 Brain imaging lesions associated with VaD (from reference 4, with modification)

		Dementia			
I	Topography	Radiological lesions associated with dementia include any of the following or combinations thereof:	A	Large-vessel strokes in the following territories:	Bilateral ACA PCA, including paramedian thalamic infarcts, inferior medial temporal lobe lesions MCA, including parietotemporal, temporooccipital territories, and/or angular gyrus Watershed carotid territories: bilateral superior frontal, parieto-occipital and/or deep and superficial MCA
			B	Small-vessel disease:	Multiple basal ganglia and frontal white matter lacunae (must be two or more lacunae in the basal ganglia and two or more lacunae in the frontal white matter) Extensive periventricular white matter lesions (as defined in IIC) Bilateral thalamic lesions
II	Severity	In addition to the above, relevant radiological lesions associated with dementia include:	A	Large-vessel lesions of the dominant hemisphere	
			B	Bilateral large-vessel hemispheric strokes	
			C	Leukoencephalopathy involving at least 25% of the total white matter (beginning to become confluent[a] in four regions, i.e., frontal bilaterally *and* parietal bilaterally)	

[a] A lesion is considered confluent when larger than 20 mm or consists of two or more smaller confluent lesions.

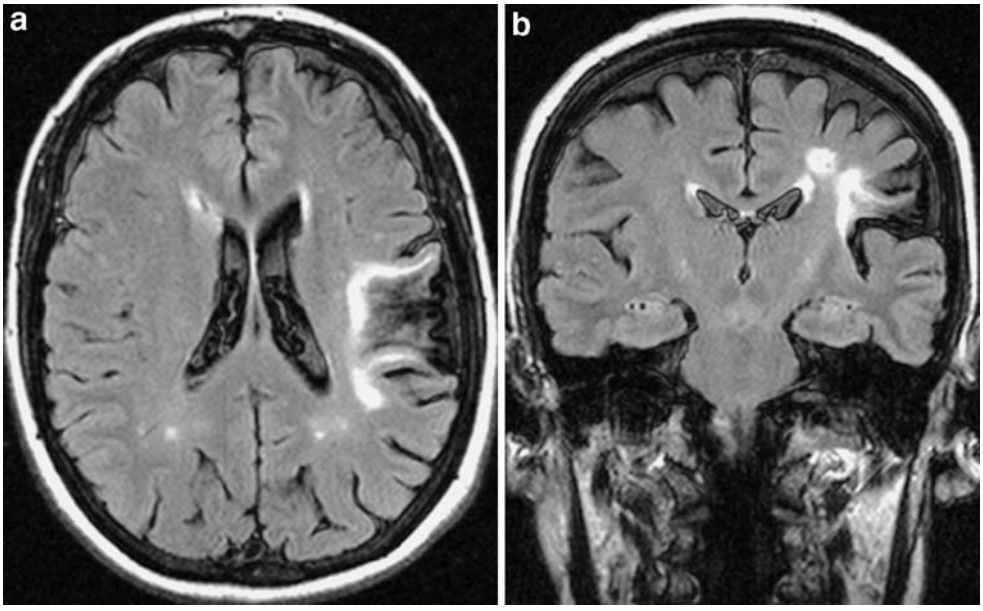

Fig. 1 Angular gyrus infarct in a 63-year-old woman with cognitive impairment. **a** Axial and **b** coronal FLAIR MR images show infarct in the left dominant angular gyrus. There are also periventricular and deep white matter hyperintensities

changes in pontine ischemic rarefaction are consistent with arteriosclerotic encephalopathy-like pathology. Pontine hyperintensity can be unilateral but in most patients is bilateral (Fig. 5). Wallerian degeneration refers to the process of anterograde degeneration of axon and its myelin sheath after connection with the cell body has been disrupted. Proton density- and T2-weighted MR images show post-stroke hyperintensity in the ipsilateral cerebral peduncle and internal capsule (Fig. 6) [29].

Watershed infarcts

Watershed infarcts are ischemic lesions that occur in the border zone regions between two or three main arterial territories (Fig. 7). The pathophysiology of watershed infarcts is controversial. Most result from hemodynamic events, usually in patients with severe internal carotid artery (ICA) stenosis or occlusion, systemic hypotension, microemboli, or a combination of these (Fig. 8) [4, 30–32].

Posterior cortical watershed infarcts are those located between the cortical supply of the MCA and PCA. They are frequently difficult to differentiate from partial territorial infarcts involving the posterior division of the MCA. Anterior cortical watershed infarcts are those located between the cortical supply of the ACA and MCA. Internal watershed infarcts are those located between the ACA, MCA, and PCA, and the area supplied by the Heubner, the lenticulostriate, and the anterior choroidal arteries. It can be

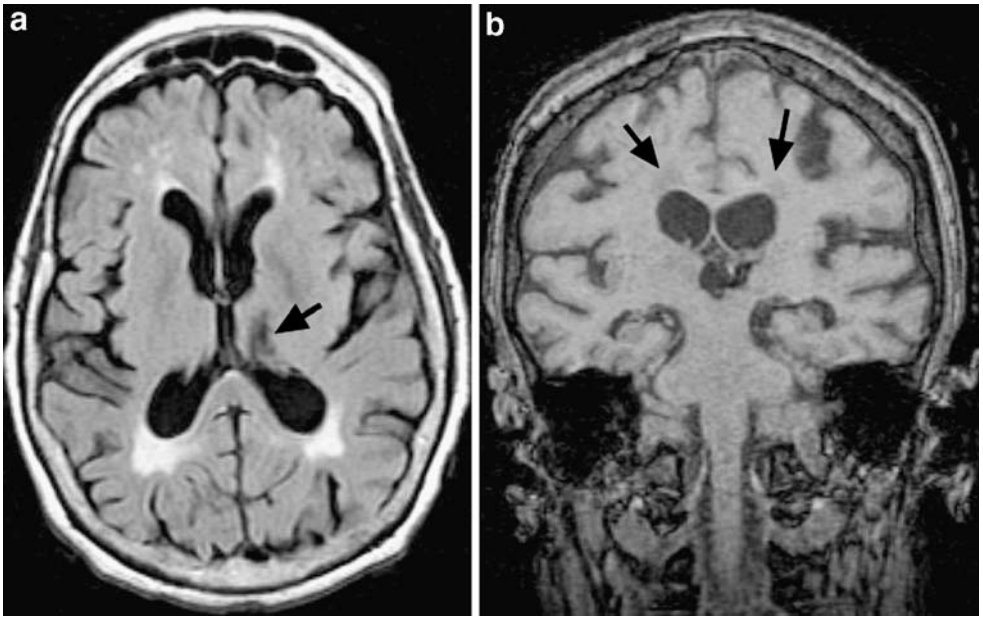

Fig. 2 Thalamic infarct in a 58-year-old man with dementia. **a** Axial FLAIR MR image shows infarct in the left dominant thalamus (*arrow*). There are also periventricular and deep white matter hyperintensities and global mild cerebral atrophy. **b** Coronal 3D SPGR T1-weighted MR image confirms the thalamic infarct and the cerebral atrophy. It also shows mild bilateral hippocampal atrophy. The white matter abnormalities are difficult to see as periventricular hypointensities (*arrows*)

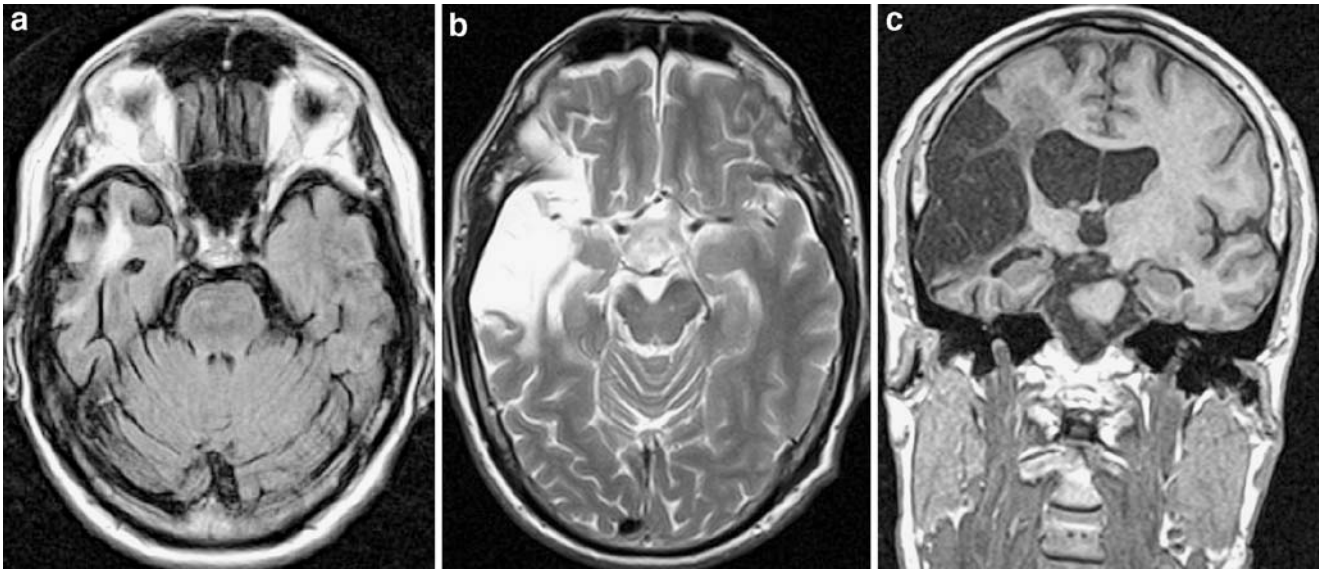

Fig. 3 Temporoparietal infarct in a 62-year-old man with dementia. Axial **a** FLAIR and **b** spin-echo T2-weighted MR images show extensive right dominant temporoparietal infarct with dilatation of the temporal horn secondary to temporal lobe atrophy. There is an atrophy of the ipsilateral right pons and mild asymmetry of the right peduncle related to Wallerian degeneration. **c** Coronal 3D SPGR T1-weighted MR image shows also an ipsilateral dilated lateral ventricle

difficult to recognize this watershed infarct from centrum ovale infarcts within the territory fed by the medullary branches of the MCA. The presence of multiple rosary-like lesions highly favors the diagnosis of watershed infarct. Watershed infarcts involving more than one of the border-zone areas in a single hemisphere are mostly related to severe ICA stenosis or occlusion. Bilateral watershed infarcts are typically related to a profound global reduction in perfusion pressure (hypoxia, hypovolemia) or to diffuse cerebral vasculopathy.

Imaging shows multiple ischemic lesions in a linear pattern in the white matter of the centrum semiovale or corona radiata, and parallel to the lateral ventricle (Figs. 9, 10, 11 and 12). This pattern is more frequently found on MRI than on CT, likely due to the superior sensitivity of MRI for depicting of white matter disease [31].

Centrum ovale infarcts can be divided into large and small infarcts, and are limited to the medullary branches without accompanying involvement of the cortex of the deep perforator artery (Fig. 13). Large centrum ovale

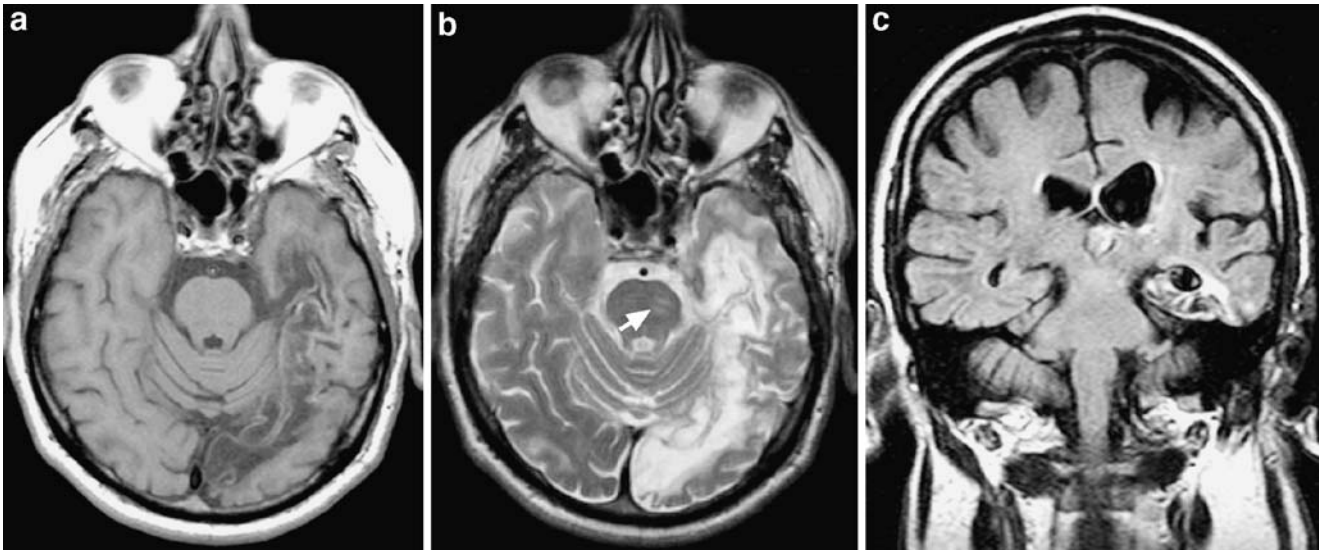

Fig. 4 Temporooccipital infarct in a 70-year-old man with dementia. Axial **a** spin-echo T1-and **b** T2-weighted MR images show extensive left dominant temporooccipital infarct. There is hyperintensity T2 in the ipsilateral pons (*arrow*) related to Wallerian degeneration. **c** Coronal FLAIR MR image shows also an ipsilateral dilated lateral ventricle with dilatation of the temporal horn secondary to temporal lobe atrophy

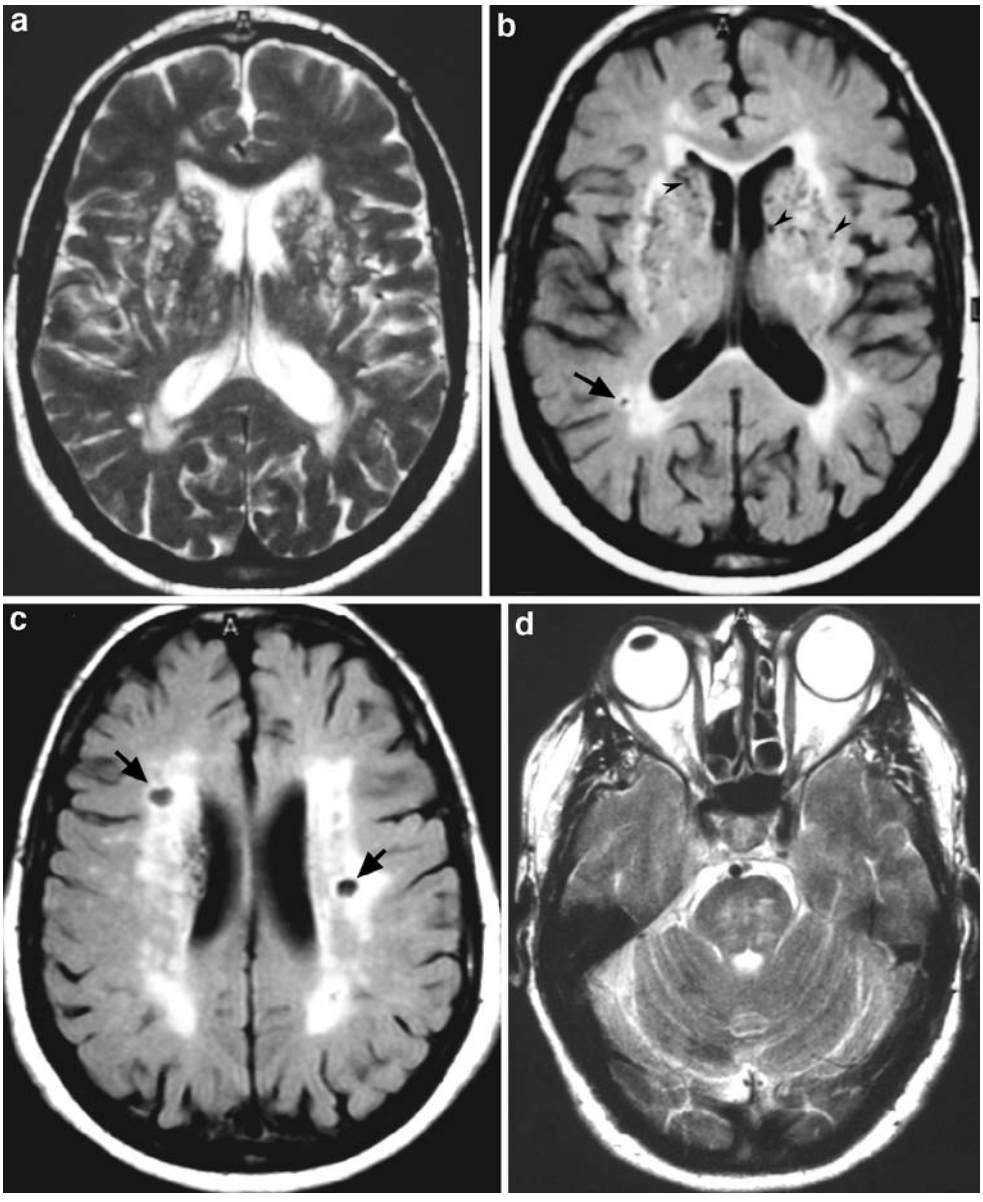

Fig. 5 Pontine ischemic rarefaction due to état criblé, white matter lesions and lacunae in a 79-year-old woman. **a** Axial spin-echo T2-weighted and **b**, **c** FLAIR MR images show widening of the perivascular spaces in the basal ganglia known as état criblé, with an extensive rim of hyperintensity involving the periventricular and lobar white matter, but sparing the U-fibers. There are small hypointense lesions in the basal ganglia (*arrowheads*) and some rather rounded hypointense lesions in the periventricular hyperintensity representing lacunar infarcts (*arrows*). **d** Axial spin-echo T2-weighted MR image at the level of the brain stem shows bilateral hyperintensity in the pons related to ischemic rarefaction

infarcts are greater than 1.5 cm and involve more than one medullary branch (Fig. 14). A hemodynamic mechanism related to ipsilateral ICA [33, 34] or MCA disease may be a leading cause of these infarcts. The infarct involves the internal border zone (between the deep perforators and superficial medullary territories of the MCA). Small centrum ovale infarcts are infarcts involving only one medullary branch (Fig. 15). They are associated with hypertension and diabetes. Multiple small rosary-like centrum ovale infarcts were thought to be related to small-vessel disease involving the medullary branches, in a manner similar to lacunar infarct [34]. However, recent studies have shown that in significant proportion of patients, small central ovale infarcts are associated with large-vessel and heart disease, and should be distinguished from the more common lacunar disease [31, 32].

Small-vessel disease

White matter abnormalities and lacunae are the hallmark lesions of cerebral small-vessel disease [35]. Multiple lacunae and a white matter lesion load of more than 10 cm^2 are likely to cause cognitive impairment [35, 36].

White matter disease

White matter high-signal foci have been called by several names, including high-signal-intensity lesions, leukoaraiosis [4], periventricular rim and caps, unidentified bright objects [37], signal hyperintensities, incidental high-signal foci, white matter lesions and white matter findings [38]. The clinical significance and pathological basis of these lesions that are frequently observed in the elderly by brain imaging

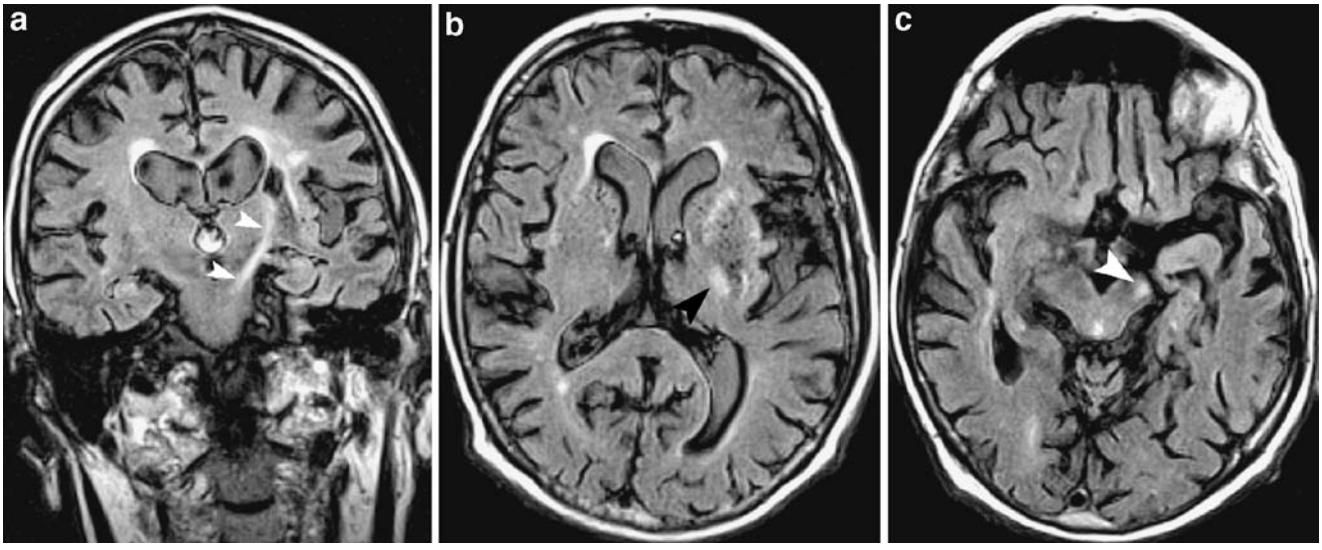

Fig. 6 Wallerian degeneration, infarct and état criblé in a 62-year-old woman with dementia. **a** Coronal and **b**, **c** axial FLAIR MR images show a left corona radiata infarct with ipsilateral dilated lateral ventricle and hyperintensity in the ipsilateral internal capsule and the cerebral peduncle which demonstrates signs of atrophy (*arrowheads*). There is also mild widening of the Virchow-Robin spaces in the basal ganglia, periventricular hyperintensities and global cerebral atrophy predominant at the left side

remain controversial [36, 39]. A number of conditions may present with patchy or diffuse white matter changes on brain imaging and require consideration in the differential diagnosis (Table 4) [4, 37, 40, 41].

Leukoaraiosis Leukoaraiosis lesions probably cause the more extensive periventricular white matter changes seen on imaging in some apparently normal elderly subjects [36, 41–43], in VaD patients [42, 44], and in some Alzheimer disease patients [4, 42, 45]. In a cross-sectional study, Guttmann et al. suggested that decreased white matter volume is age-related, whereas increased white matter signal abnormalities are most likely to occur as a result of disease [42, 46]. Among several causes of this leukoencephalopathy, morphological changes in the wall of perforating arteries, including elongation and tortuosity of vessels in the elderly and hypoperfusion and ischemia resulting from arteriosclerosis are the more probable [4]. Periventricular leukoaraiosis seen on CT or MRI alone may be considered evidence of cerebrovascular disease with widespread incomplete infarct of deep white matter, with a clinical picture of Binswanger disease [2, 47]. (The term "leukoaraiosis" is often used interchangeably with "Binswanger disease", but the use of this term should be discouraged since "leukoaraiosis is neither a disease nor even a specific indicator for white matter ischemia" [48].) These incomplete or non-cavitating ischemic white matter lesions of the brain are common in elderly people. In a study of 3,301 patients, only 4.4% did not have white matter lesions with findings more common among those without a history of stroke. In approximately 80% of patients, the findings were mild, with little clinical significance. White matter lesions are periventricular and/or subcortical. They are most commonly symmetrical, supratentorial and periventricular [49], but also less commonly infratentorial [44].

Boone et al. have suggested that a threshold of white matter area greater than 10 cm^2 is almost always reached

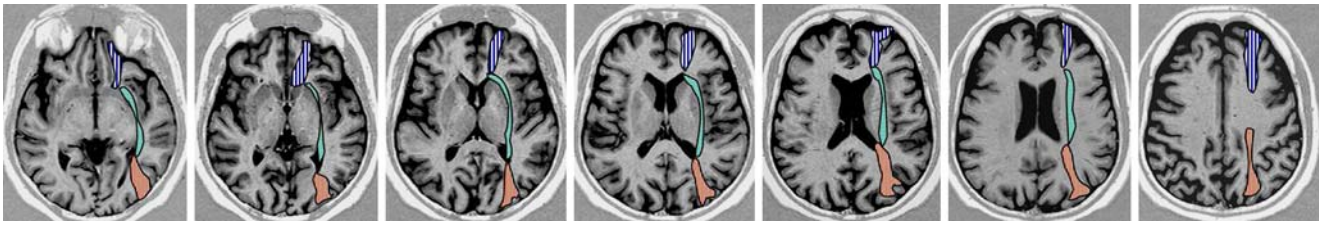

Fig. 7 Drawing showing the topographical pattern of cerebral watershed infarcts. Posterior cortical watershed infarcts (*red*) are those located between the cortical supply of the MCA and PCA. They are frequently difficult to differentiate from partial territorial infarcts involving the posterior division of the MCA. Anterior cortical watershed infarcts (*blue*) are those located between the cortical supply of the ACA and MCA. Internal watershed infarcts (*green*) are those located between the ACA, MCA, and PCA, and the area supplied by the Heubner, the lenticulostriate, and the anterior choroidal arteries

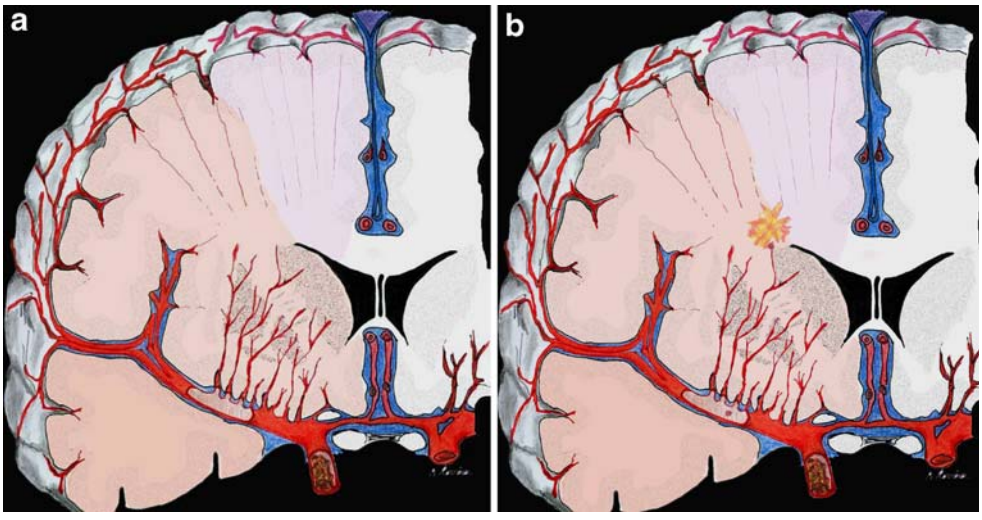

Fig. 8 Drawing showing **a** a hemodynamic cortical watershed infarct affecting the border zone area between the MCA and ACA territories and **b** an internal watershed infarct due to arrival of microemboli through the MCA deep perforators. Thus, a double mechanism, embolic and hemodynamic, may produce this type of infarct

before cognitive deficits are observed [36]. Nevertheless, in clinical trials, the decision was made to consider the total volume of white matter changes rather than trying to grade specific findings, and a rating scale for the location and severity of these changes has been developed [50]. Indeed, these changes should be diffuse and extensive, and involve at least 25% of the total white matter to be considered VaD-related [2, 50]. However, this portion is set purely arbitrarily and a practicable and clinically valid rating scale has to be used. Several visual scales have been developed that are applicable to both CT and MRI and give an estimate of vascular burden with acceptable reliability (Table 5) [42, 44, 51]. The ideal rating scale would be the one which, besides including the anatomical distribution, makes a clear and practical distinction between periventricular and deep white matter changes. The trend is for more refined techniques, such as semiautomated segmentation which will replace visual rating in the future [50].

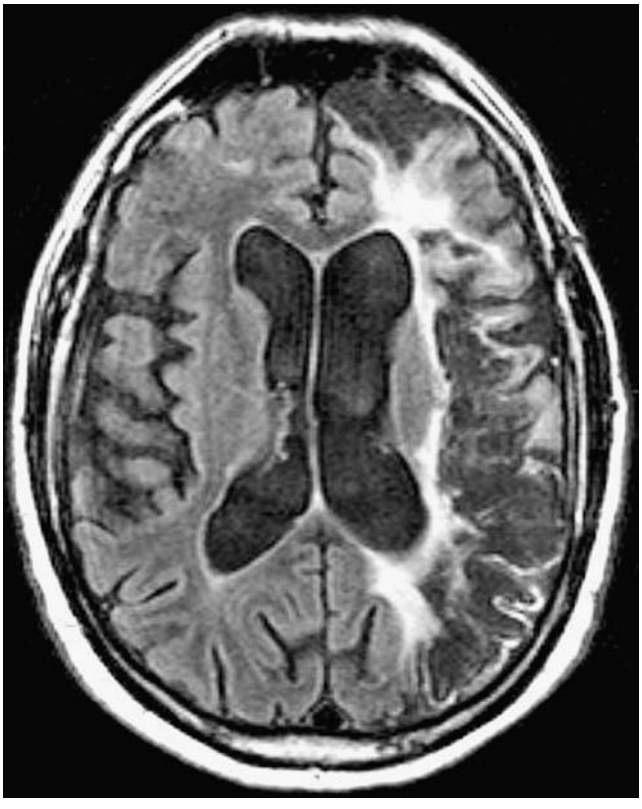

Fig. 9 Extensive superficial MCA and anterior and posterior watershed infarcts in a 58-year-old man with dementia. Axial FLAIR MR image shows an extensive left superficial MCA infarct, associated with anterior and posterior cortical watershed infarcts. There is a surrounding hyperintensity due to gliosis, an ipsilateral dilated lateral ventricle, and global cerebral atrophy

White matter changes are seen as patchy or diffuse symmetrical areas of hypodensity or intermediate density on CT (Fig. 18) [2]. On MRI, they are characterized by periventricular hypointensity on T1-weighted, and hyperintensity on proton density-weighted, T2-weighted and FLAIR images, extending to the deep white matter but sparing the areas thought to be protected from perfusion insufficiency, such as subcortical U-fibers (Fig. 19). Changes observed only on T2-weighted images may be insignificant [4]. They can be distinguished from territorial infarcts by their lack of correspondence with a specific vascular territory, well-defined margins, lack of wedge shape, lack of cortical involvement, and association with enlarged ipsilateral sulci and ventricles. The abnormalities detected by CT and MRI are not identical in terms of number, site, or extension [52]. There is good interobserver agreement on visual scales, but different scales attribute different significance to the same radiological picture [50]. MRI is more sensitive than CT for detection of white matter lesions [2]. In terms of MRI sequences, T2-weighted images show more small foci than proton density- and T1-weighted images. This is understandable since T2-weighted images are sensitive to liquid, gliosis or effects of demyelination. Proton density-weighted images proved more sensitive than T2-weighted or T1-weighted images for

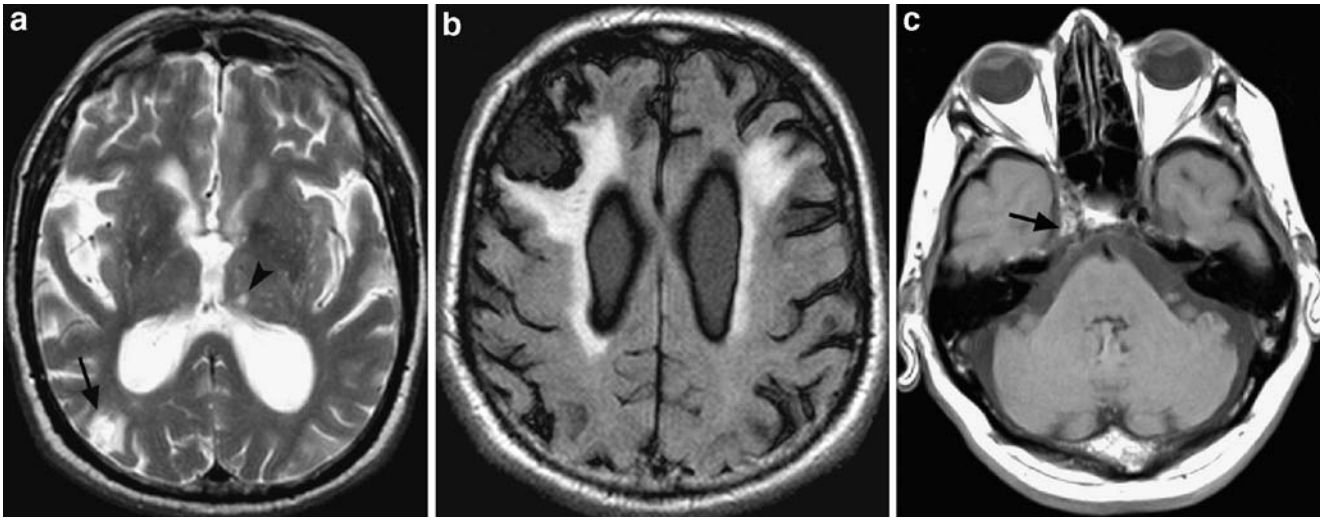

Fig. 10 Watershed infarcts in a 65-year-old woman with cognitive impairment. **a** Axial spin-echo T2-weighted MR image shows right posterior cortical watershed infarct (*arrow*) and small left thalamic lacuna (*arrowhead*). **b** Axial FLAIR MR image shows a right anterior cortical watershed infarct and periventricular white matter hyperintensities. **c** Axial T1-weighted MR image shows thrombosis of the right ICA (*arrow*). This patient was considered to have possible VaD because the watershed infarcts and thalamic lacuna were unilateral. The white matter involvement did not exceed 25%

the detection of small periventricular foci. This is also understandable, since periventricular high signal is usually very close to the hyperintensity of cerebrospinal fluid in the ventricles on T2-weighted images. FLAIR images proved most sensitive as T1-weighted images proved least sensitive, as was to be expected. However, it is noteworthy that a considerable part of the signal change detected on T2-weighted and proton density-weighted images could be seen also on T1-weighted images [38].

Cerebral autosomal dominant arteriopathy with subcortical infarcts and leukoencephalopathy (CADASIL) CADASIL is considered a familial form of Binswanger disease presenting in younger patients in the absence of vascular risk factors [48]. It is a condition characterized by recurrent strokes, with stepwise progression of neurological deficits and, ultimately, dementia and severe motor disability. The disease locus has been assigned to chromosome 19q12 [2]. Imaging may show two main abnormalities. First, 0.5 to 2 cm linear or punctate sharply defined lesions that are consistent with small infarcts in the periventricular deep white matter, subcortical white matter, external capsule, brain stem, basal ganglia and thalamus. MR images actually show small infarcts, some of which may become lacunar. Second, large, confluent patches of abnormal tissue appear in subcortical regions; they are often symmetrical and tend

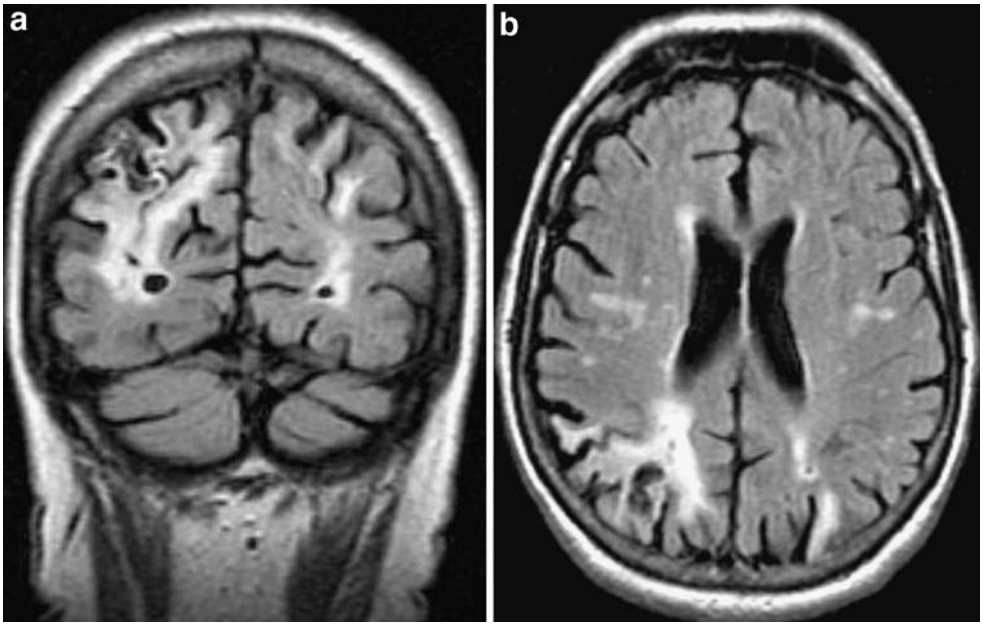

Fig. 11 Bilateral posterior watershed infarcts in a 71-year-old woman with dementia. **a** Coronal and **b** axial FLAIR show bilateral posterior cortical watershed infarcts. There are also several spots of deep white matter hyperintensities. This patient was considered to have probable VaD by NINDS-AIREN criteria

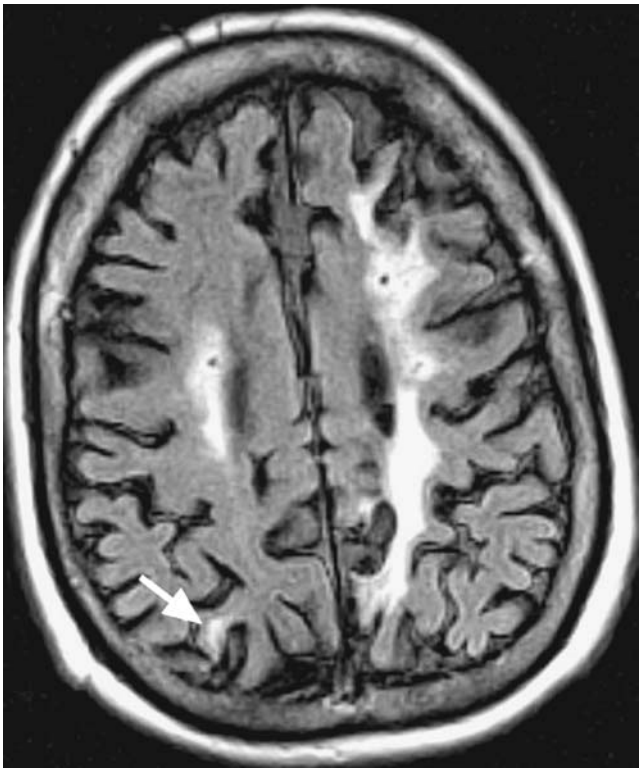

Fig. 12 Bilateral watershed infarcts in 69-year-old man with dementia. Axial FLAIR MR image shows watershed infarcts involving all three left border zone areas and right posterior cortical (*arrow*) and internal border zone areas. This patient was considered to have probable VaD by NINDS-AIREN criteria

to occur in the anterior part of the temporal lobes and the periventricular portion of the occipital lobe. The patches of abnormal tissue are best seen on MR images, and are hypointense on T1-weighted images and hyperintense on proton density- and T2-weighted images [53, 54]. Temporal white matter involvement is the major finding differentiating CADASIL from Binswanger disease (Fig. 20). Paramedian superior frontal white matter regions and arcuate fiber involvement are also other useful signs that help to differentiate CADASIL from Binswanger disease [54]. Areas of low signal intensity on T2-weighted and FLAIR images within the deep gray matter nuclei are interpreted as increased iron deposition, possibly resulting from disturbed axonal iron transport [54].

Amyloid angiopathy Amyloid angiopathy is a hereditary form of small-vessel disease [55]. It is characterized by single or more frequently multiple lobar nontraumatic hemorrhage [56] located, with decreasing frequency, in the frontal, parietal, temporal and occipital lobes. Cerebellar and basal ganglia hemorrhages are infrequent and brain stem hemorrhages are extremely rare. Sporadic forms may present with a variety of symptoms other than lobar hemorrhage, including petechial hemorrhage in cortical and subcortical areas, and they may produce rapid and progressive dementia. MRI will show more detail and infarcts, when present, than CT. In most cases MRI will show severe white matter involvement with confluent and isolated lesions [57]. Gradient-echo MRI sequences show multiple areas, often dispersed through the brain, with very low signal intensity due to locally changed magnetic susceptibility (Fig. 21). These lesions, which are related to intracranial hemorrhage, are usually not seen on CT, or FLAIR, or spin-echo T2-weighted, T1-weighted and proton density-weighted MRI, certainly not with the same conspicuity as with gradient echo T2-weighted MRI [58].

Lacunar strokes or lacunar infarcts or lacunae or lacunar state

Lacunae are common small deep infarcts of the brain of less than 2 cm in size, are single or multiple, are clinically silent, or less frequently, symptomatic [59]. Lacunae result from small-vessel disease with lumen occlusion secondary to arteriolosclerosis due to microatheroma and lipohyalinosis, or embolism, usually in patients with arterial hypertension. Lacunae are located in a territory supplied

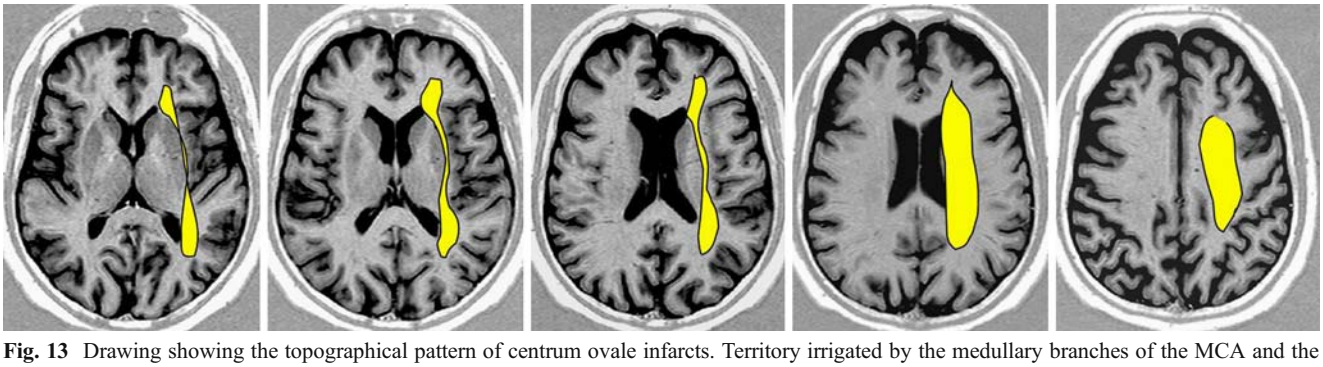

Fig. 13 Drawing showing the topographical pattern of centrum ovale infarcts. Territory irrigated by the medullary branches of the MCA and the anterior choroidal arteries is colored in *yellow*

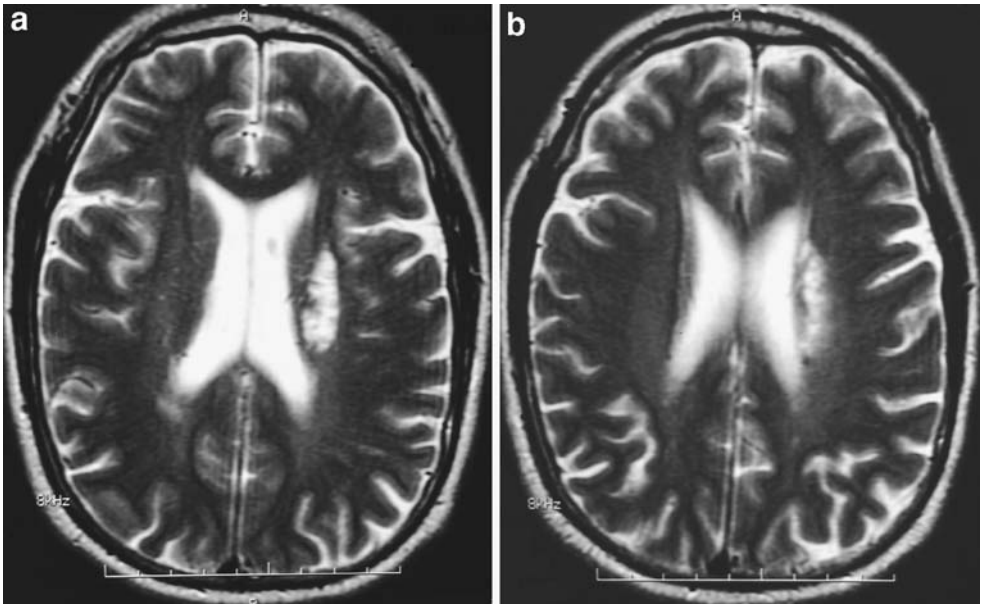

Fig. 14 Large centrum ovale infarct in a 56-year-old man with dementia. **a**, **b** Axial spin-echo T2-weighted MR images show a large infarct involving the left central white matter. There are also caps of white matter hyperintensities around the posterior horn of the lateral ventricles

by the deep perforators such as lenticulostriate, thalamoperforating, and long medullary arterioles (Fig. 22) [60]. Therefore, lacunae can be located in the basal ganglia, the upper two-thirds of the putamen, the internal capsule, the thalamus, the paramedian and lateral regions of the brain stem (pontine base) (Fig. 23), corona radiata, and centrum semiovale [2, 4]. Special attention needs to be paid to the thalamus, which plays a role in several aspects of cognition. Indeed, damage to this structure, even small and/or unilateral, may affect memory, executive functioning and attention (Fig. 24) [61, 62].

Lacunae must be distinguished from dilated perivenricular spaces (état criblé) [63]. Lacunae are round, oval, or slit-like, small cavitated ischemic brain infarcts measuring up to 1.5 cm in maximum diameter, and resulting in a lacunar state or état lacunaire [2, 59]. A limit of 3–20 mm is generally used in radiological studies. Lacunar infarcts are hypodense on CT scans, hypointense on T1-weighted MRI, and hyperintense on proton density- and T2-weighted MRI (Fig. 24) [60]. Thalamic lesions (as well as infratentorial lesions) are best seen on T2-weighted images, and sometimes missed on FLAIR images [64]. Small old hemorrhages have the same appearance as lacunar infarcts on CT scans but their centers appear hypointense on proton density- and T2-weighted MRI due to hemosiderin deposition [60]. In practice, lacunae and deep white matter lesions, the two forms of subcortical ischemic VaD, are often seen together, presumably because of their common origin [2].

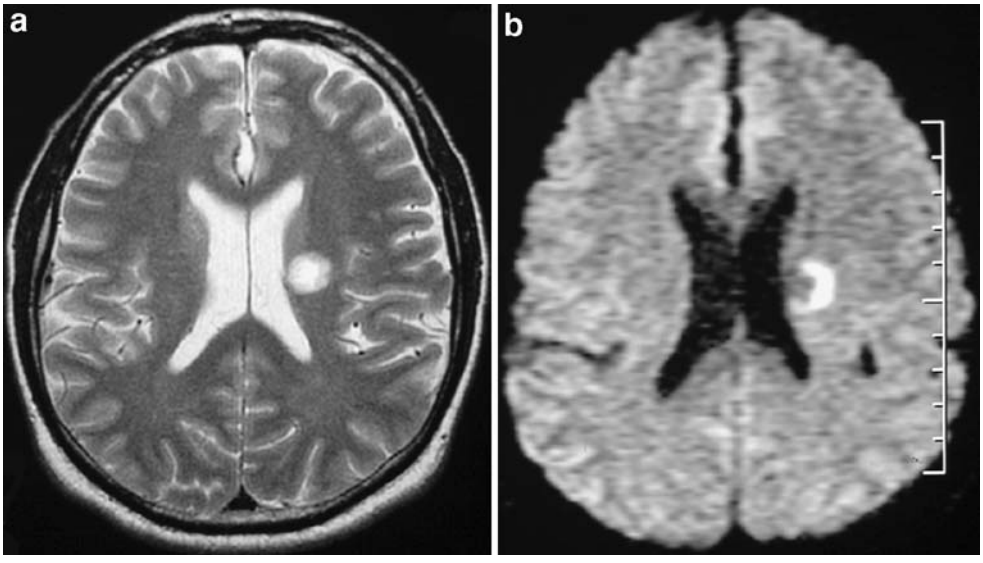

Fig. 15 Small central ovale infarct in a 53-year-old man with dementia. Axial **a** spin-echo T2-weighted and **b** diffusion-weighted MR images show a solitary small rounded infarct involving the left central white matter. Because only one small infarct was detected in this patient, he was considered to have possible VaD by NINDS-AIREN criteria

Table 4 Diseases with patchy or diffuse white matter lesions on brain imaging [4]

Conditions
Senile leukoencephalopathy (leukoaraiosis)
Leukodystrophies with defective myelination
Adrenoleukodystrophy, globoid cell dystrophy, metachromatic leukodystrophy
Hemodynamic disorders
Neonatal anoxia, hypoxia-ischemia, cardiopulmonary arrest
Posterior reversible encephalopathy syndrome (PRES) (Fig. 16)
Subarachnoid hemorrhage
Arteriovenous malformations
Cerebral amyloid angiopathy
Cerebral autosomal dominant arteriopathy with subcortical infarcts and leukoencephalopathy (CADASIL)
Cerebral venous thrombosis
Polycythemia
Cerebral edema
Recent stroke, trauma, metastases
Hydrocephalus
Obstructive, normal-pressure hydrocephalus
Brain irradiation
Methotrexate intrathecal treatment
Encephalitides
Subacute sclerosing panencephalitis, progressive multifocal leukoencephalopathy, HIV encephalopathy, other infections, systemic lupus erythematosus, temporal arteritis, acute disseminated encephalomyelitis (ADEM), other inflammatory and noninflammatory arteriopathies
Neurosarcoidosis
Multiple sclerosis (Fig. 17)
Alzheimer disease
Binswanger disease
Creutzfeldt-Jakob disease
Other conditions
Hepatic coma, uremia, hypoglycemia, gangliodoses, mucopolysaccharidoses

Dilatation of perivascular spaces or état criblé

Microscopically, perivascular spaces, also called Virchow-Robin spaces, have a small vessel within the lacuna and show no evidence of necrosis, macrophages, or tissue debris (Fig. 25) [65]. Widened perivascular spaces are the hallmark of the condition known as état criblé (Figs. 5 and 6). This condition is thought to be limited to the basal ganglia and therefore to the gray matter nuclei. They are reported to be significantly associated with age, hypertension, dementia, and incidental white matter lesions [66]. Enlarged perivascular spaces appear as single or multiple cerebrospinal fluid isointense lesions on all sequences, especially proton density-weighted MRI. They are clearly demarcated round or linear lesions, usually bilateral, but may be unilateral, and are localized at the level of anterior commissure, basal ganglia, cerebral convexity, midbrain, or inferior putamen and are smaller than 1×2 mm in area. In the inferior putamen, they are also called infraputaminal lacunae [67–70]. High-resolution MRI has shown that in quite a few patients pseudoconfluent white matter changes, in particular in the peritrigonal areas, as seen on lower-resolution MRI and CT (Fig. 26), dissolve into widened Virchow-Robin spaces. They may be misdiagnosed as lacunar infarcts, which are frequent in the basal ganglia and are round, oval or slit-like in morphology [67]. But unlike infarcts, these fluid-filled lesions are isointense to cerebrospinal fluid on proton density-weighted images [68, 71] and also on FLAIR sequences [67]. They are usually asymptomatic [68]. On rare occasions spontaneous single or widespread dilatation of Virchow-Robin spaces may produce neurological deficits by local pressure effects [68] and may also be associated with subcortical VaD [72, 73]. When they present as expanding lacunae [71], they may also rarely cause triventricular hydrocephalus [74]. Nevertheless, there was no evidence of local mass effect in any of the patients reported in the literature on either imaging or at autopsy [68]. Enlarged perivascular spaces of the extreme capsule and insular cortex are seen as high signal intensity subinsular foci at MRI. They are best seen on coronal images as elliptical, round, linear or dot-like, often have a feather-like configuration and should not be mistaken for pathological conditions when they occur unilaterally [69].

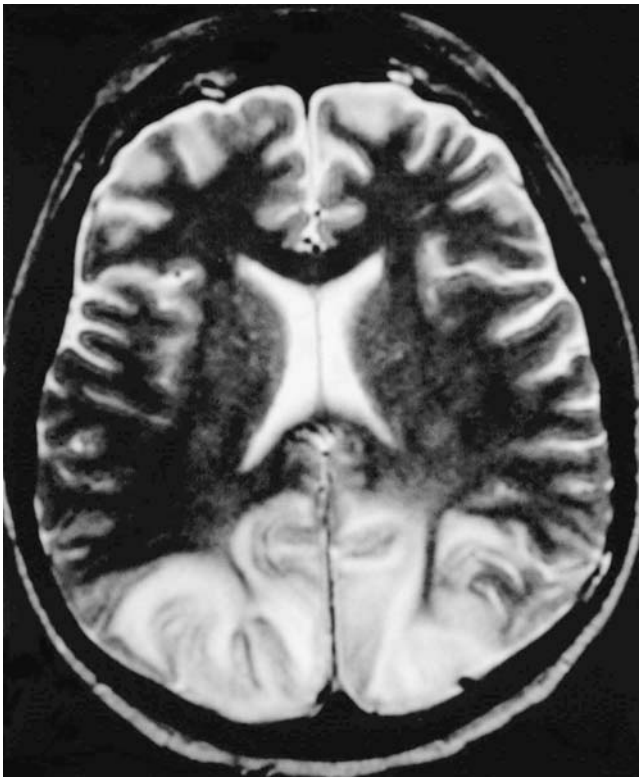

Fig. 16 Posterior reversible encephalopathy syndrome (PRES) in a 52-year-old man with cognitive impairment and visual disturbance. Axial spin-echo T2-weighted MR image shows bilateral hyperintense parietooccipital signal abnormalities involving the cortex and subcortical white matter. These abnormalities are related to cyclosporine toxicity. MR images returned to normal within 10 days

Cerebral atrophy

VaD features hippocampal atrophy less severely than Alzheimer disease, in addition to cortical and/or subcortical signs of vascular damage [75]. The severity of dementia in subcortical VaD correlates more strongly with the degree of hippocampal (Fig. 2) and cerebral atrophy than with severity of white matter hyperintensities [28, 76]. Nonetheless, cerebral atrophy and white matter lesions are related. Comparison between healthy elderly individuals and patients with VaD shows clear evidence of disease-related patterns of atrophy (Fig. 27) [77], as is the case with Alzheimer disease and dementia with Lewy bodies [78]. Patients with VaD have proportionately greater degrees of atrophy in the middle of the CSF space compared with that in the back of the CSF space than is seen in patients with Alzheimer disease and healthy elderly patients [77]. Quantitative MRI reveals widespread atrophy in subcortical ischemic VaD that is not solely due to focal infarct. Possible causes include cortical hypometabolism and hypoperfusion [2]. A recent study aiming to measure prospectively brain atrophy from serial MRI showed that the atrophy rate is increased in VaD, but also Alzheimer disease and dementia with Lewy bodies, in comparison with control subjects [78].

Callosal atrophy has been shown in VaD (Fig. 27) [79]. In patients with cognitive impairment related to severe white matter damage, corpus callosum atrophy, which may result from axonal disruption due to white matter changes, may be an important predictor of global cognitive decline [80].

Diagnosis exclusion

The traditional view that imaging is important solely as a means of excluding treatable causes of dementia is maintained by many guidelines. These conditions, however, account for a tiny proportion (less than 1%) of all causes of dementia. The different pathological processes that produce cerebral dysfunction at a cellular level also produce macroscopic effects that can be detected in vivo with imaging. Regardless of the criteria used for the diagnosis of VaD, neuroimaging in general, and MRI in particular, are increasingly regarded as a mandatory part of the investiga-

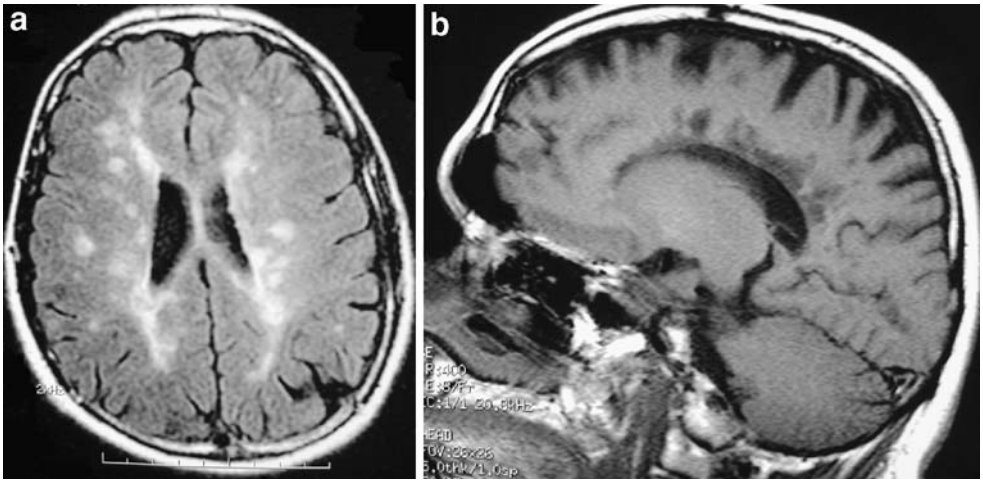

Fig. 17 Multiple sclerosis in a 44-year-old man with cognitive impairment and motor weakness. **a** Axial FLAIR MR image shows multiple hyperintense lesions clustering around the ventricles and deep white matter. **b** Sagittal T1-weighted MR image shows typical orientation of these lesions perpendicular to the lateral ventricle axis with finger-like extensions into the adjacent white matter

Table 5 Semiquantitative visual rating of signal hyperintensities by MRI [45] (*n* number of lesions)

Lesions	Score	
Periventricular hyperintensities (0–6)	0	Absent
Frontal caps (0–2)	1	≤5 mm
Occipital caps (0–2)	2	>5 mm and <10 mm
Lateral ventricle bands (0–2)		
White matter hyperintensities (0–24)	0	No abnormality
Frontal (0–6)	1	<3 mm; $n \leq 5$
Parietal (0–6)	2	<3 mm; $n > 6$
Occipital (0–6)	3	4–10 mm; $n \leq 5$
Temporal (0–6)	4	4 mm; $n > 6$
	5	>11 mm; $n > 1$
	6	Confluent
Basal ganglia hyperintensities (0–30)	0	No abnormality
Caudate nucleus (0–6)	1	<3 mm; $n \leq 5$
Putamen (0–6)	2	<3 mm; $n > 6$
Globus pallidus (0–6)	3	4–10 mm; $n \leq 5$
Thalamus (0–6)	4	4 mm; $n > 6$
Internal capsule (0–6)	5	>11 mm; $n > 1$
	6	Confluent
Infra-tentorial foci of hyperintensity (0–24)	0	No abnormality
Cerebellum (0–6)	1	<3 mm; $n \leq 5$
Mesencephalon (0–6)	2	<3 mm; $n > 6$
Pons (0–6)	3	4–10 mm; $n \leq 5$
Medulla (0–6)	4	4 mm; $n > 6$
	5	>11 mm; $n > 1$
	6	Confluent

tion of a patient with dementia. Indeed, imaging is used to exclude other abnormalities that are potentially amenable to treatment, such as tumor (Fig. 28), subdural hematoma (Fig. 29), or hydrocephalus. The sensitivity of MRI to vascular pathology has boosted research into, and clinical recognition of, VaD and has aided tremendously in distinguishing between Alzheimer disease and VaD. Indeed, the ability of MRI to detect even subtle atrophy of the medial temporal lobe helps to diagnose Alzheimer disease. However, there are possible overlap syndromes between the

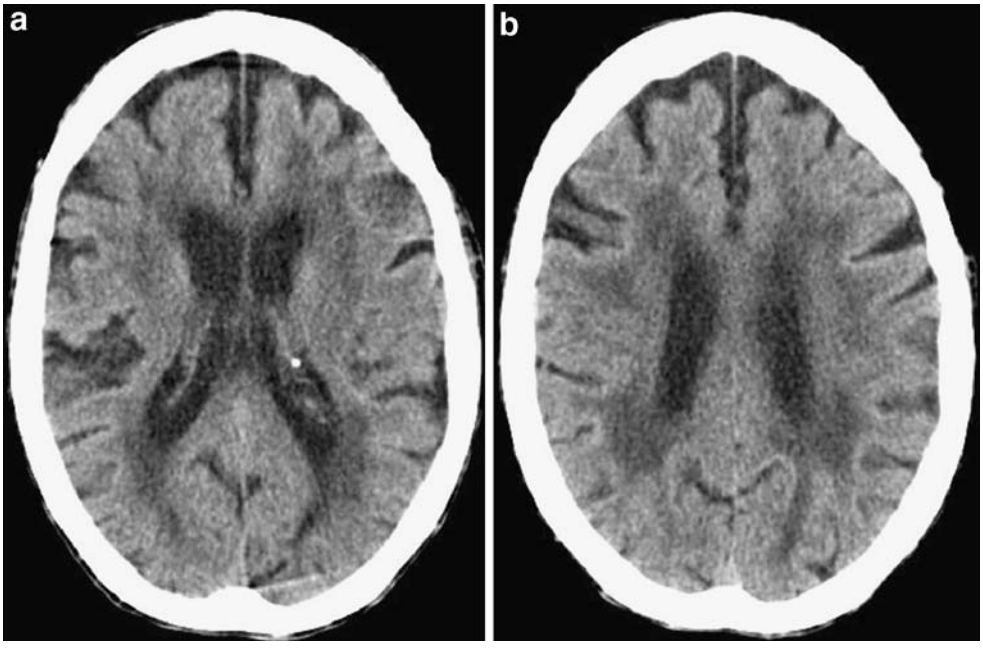

Fig. 18 Binswanger disease in a 67-year-old man with dementia. **a**, **b** Axial CT scans show extensive symmetrical hypodensity involving periventricular and lobar white matter. This diffuse involvement was considered >25% of the total white matter. There is also an important global cerebral atrophy

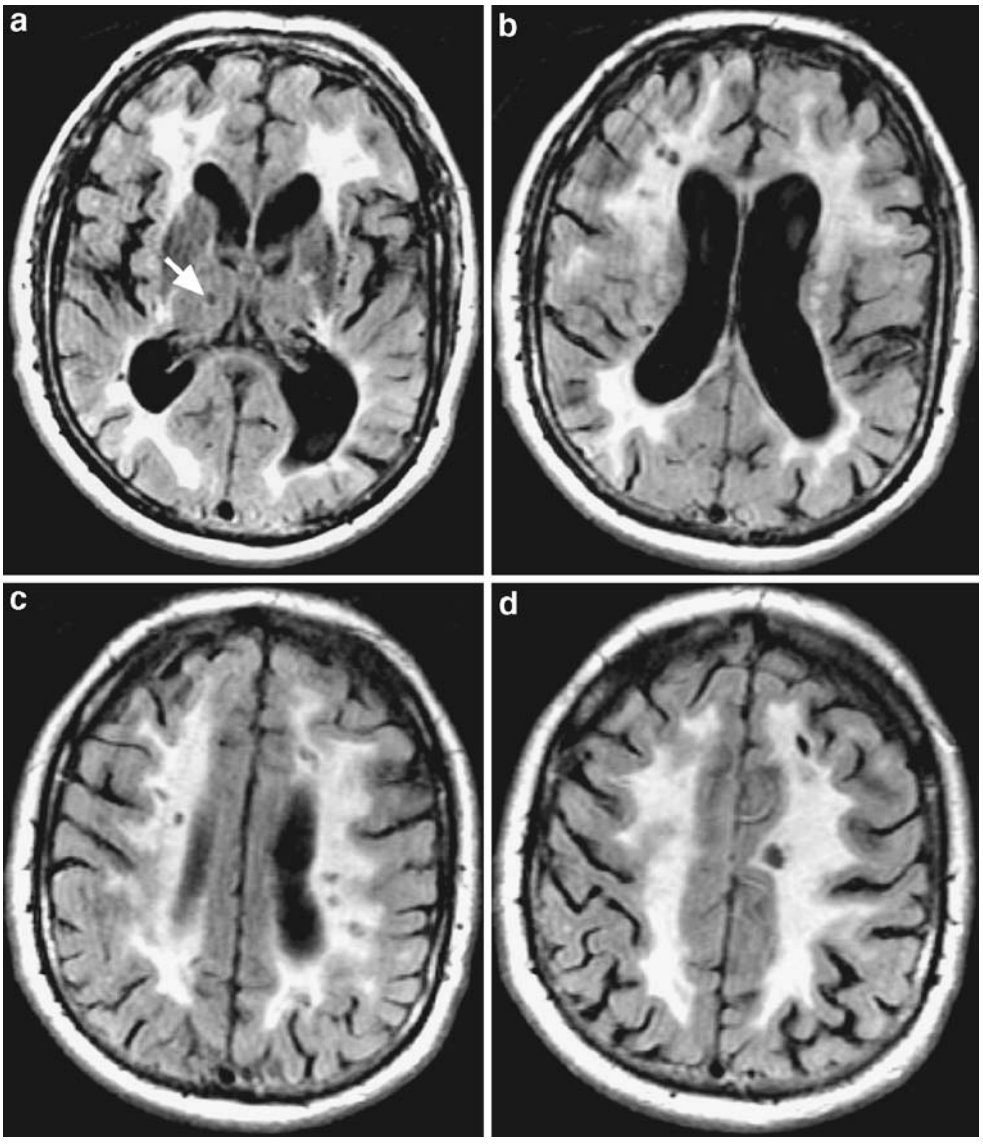

Fig. 19 Binswanger disease in an 85-year-old man with dementia. **a**–**d** Axial FLAIR MR images show extensive symmetrical hyperintensity involving periventricular and lobar white matter. These lesions have a rather sharp outer border and show sparing of the U-fibers. This diffuse involvement was considered >25% of the total white matter. There are also a lacunar right thalamic infarct (*arrow*), several bilateral hypointense lesions within the periventricular hyperintensity representing lacunar infarcts and an important global cerebral atrophy

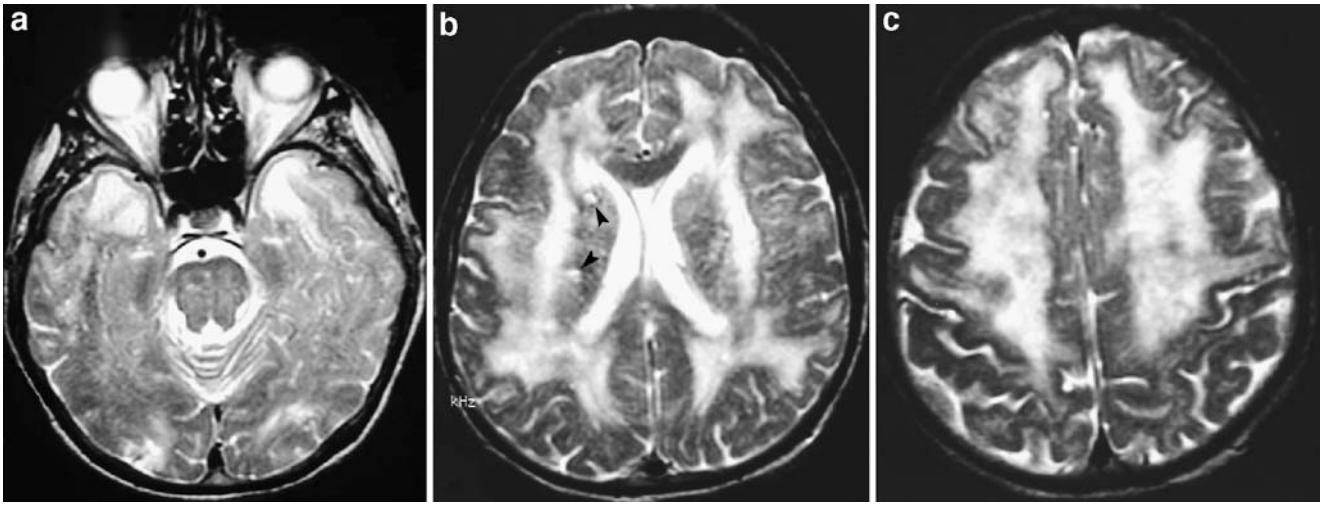

Fig. 20 CADASIL in a 57-year-old man with cognitive impairment. Axial spin-echo T2-weighted MR images show **a** extensive white matter abnormalities with characteristic symmetrical involvement of the anterior part of the temporal lobes, and **b** external and extreme capsules without involvement of the internal capsules. They also show **c** extensive white matter changes in the centrum ovale, extending towards the cortex in some places. There are also two small lacunar infarcts in the right basal ganglia (*arrowheads*)

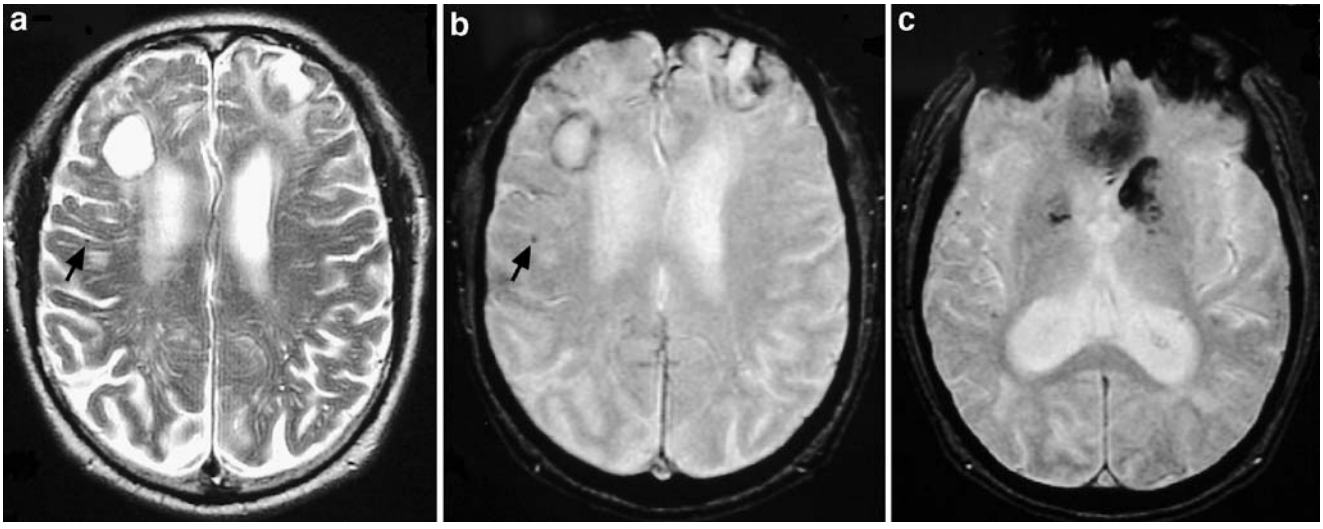

Fig. 21 Amyloid angiopathy in a 66-year-old man with dementia. **a** Axial spin-echo T2-weighted MR image shows bilateral large frontal hemorrhages surrounded by a rim of hypointensity due to hemosiderin deposition. There is also another right frontal punctate hypointense lesion (*arrow*), best seen on **b** axial the gradient-echo T2-weighted MR image. **c** Axial gradient-echo T2-weighted MR image caudal to **b** shows additional hypointensities bilaterally in the basal ganglia and the right parietal lobe

two disorders, and operational definitions for "mixed" dementia, indicating the presence of both Alzheimer disease and VaD, are still lacking [25].

Positron emission tomography (PET) has been tested for differentiation between VaD and Alzheimer disease. It shows that regional cerebral flow is significantly decreased in the parietal and temporal cortex in patients with Alzheimer disease, but not in any areas of those with VaD. On the other hand, PET shows no difference between the two entities when investigating oxygen extraction fraction [81]. A recent study using proton magnetic resonance spectroscopy (MRS) has reinforced the specific association between reduced *N*-acetyl aspartate and increased *myo*-inositol levels in the parietal occipital region and cognitive impairment in Alzheimer disease, and hence may also help differentiate this disease from VaD since the latter did not show a correlation between any of the metabolite ratios measured and cognitive impairment [82].

Treatment

So far there is no standard treatment for VaD, and still little is known about primary prevention (brain at risk for cerebrovascular disease) and secondary prevention (cerebrovascular disease brain at risk for VaD). Recently symptomatic cholinergic treatment has shown promise in Alzheimer disease and VaD [1, 24], as has an uncompetitive *N*-methyl-D-aspartate antagonist in patients with mild to moderate VaD [83].

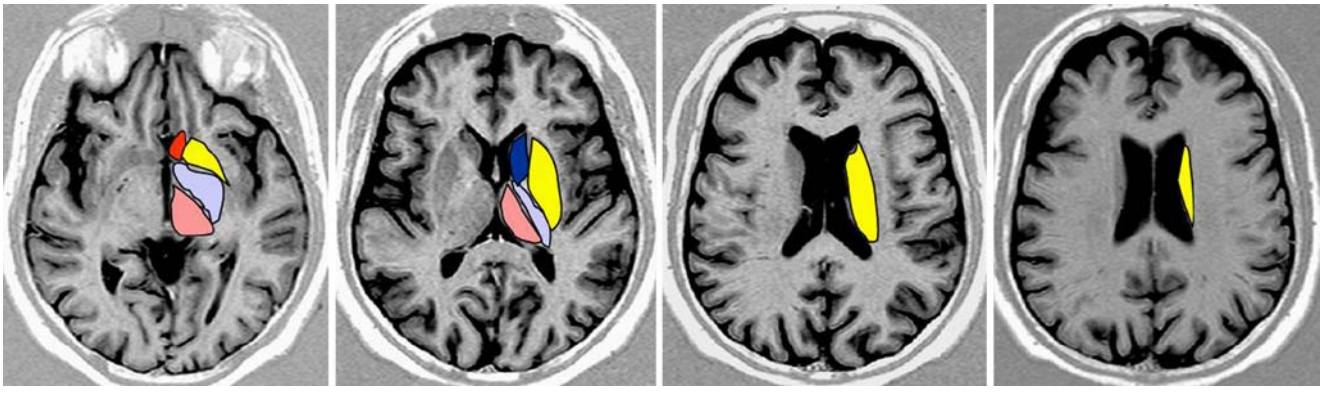

Fig. 22 Drawing showing the territory of the deep brain perforators. Heubner artery (ACA) (*red*), lenticulostriatal arteries (MCA) (*yellow*), lenticulostriatal arteries (ACA) (*blue*), anterior choroidal artery (ICA) (*mauve*), thalamoperforate arteries (PCA) (*pink*)

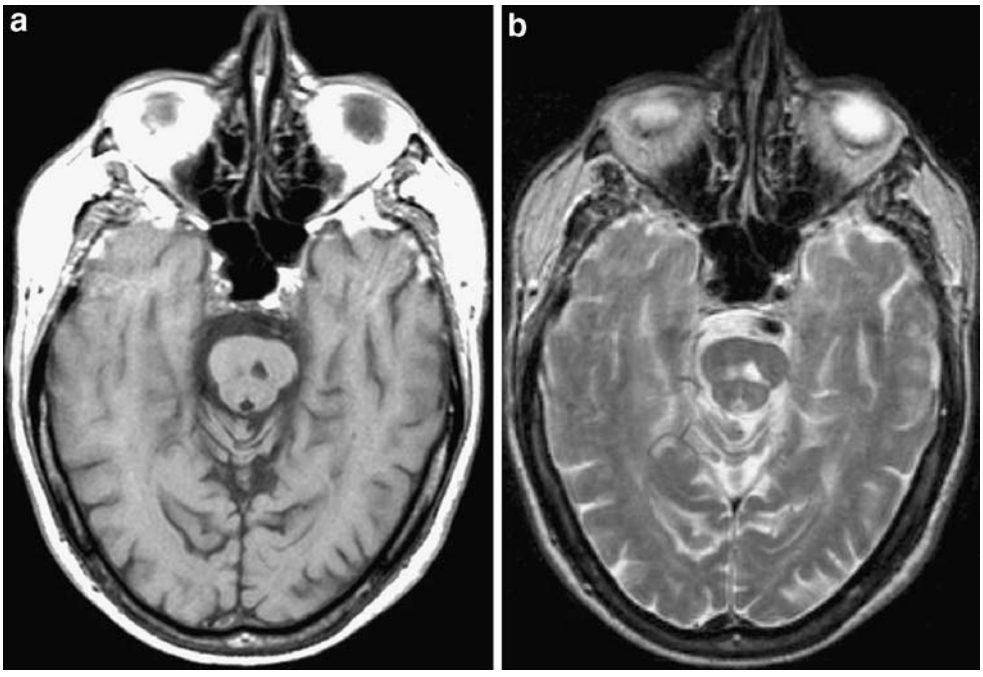

Fig. 23 Pontine lacuna in a 67-year-old woman with dementia. **a** Axial T1-weighted MR image shows an oval small hypointense lesion in the left pontine base, which appears hyperintense on **b** axial spin-echo T2-weighted MRI. This lesion corresponds to a lacunar infarct

Conclusion

VaD is a leading cause of dementia worldwide, second only to Alzheimer disease in incidence and prevalence. Current diagnostic criteria for VaD are not interchangeable and their sensitivity and specificity are variable. Furthermore, none of them can distinguish the mixed form of dementia, and the differential diagnosis between VaD and Alzheimer disease remains clinically challenging. Nevertheless, the NINDS-AIREN criteria are highly specific, excluding 91% of patients with Alzheimer disease [84]. These clinical criteria for the diagnosis of patients with VaD are now widely accepted despite their heterogeneity. Brain imaging is essential for the diagnosis and should always be performed, preferably using MRI. The place of perfusion MRI, MRS, and PET in the diagnosis of VaD is to be determined in the near future. Neuroimaging should demonstrate abnormalities consistent with cerebrovascular

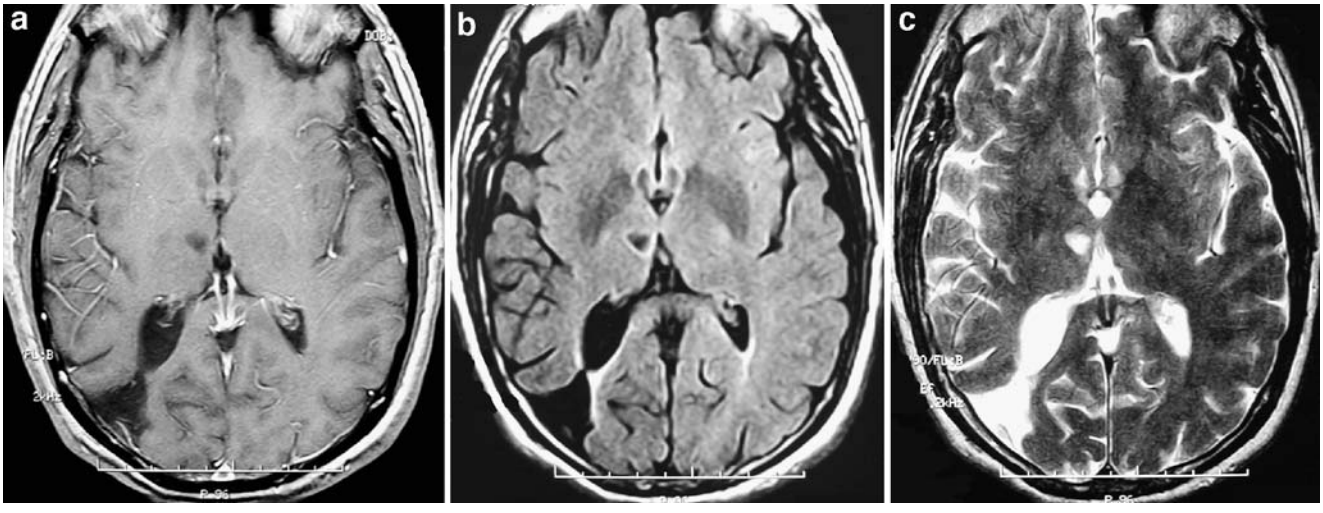

Fig. 24 Thalamic lacunar and posterior cortical watershed infarcts in a 62-year-old man with dementia. Axial **a** T1-weigthed and **b** FLAIR MR images show an oval small right thalamic hypointense lesion, which appears hyperintense on **c** axial spin-echo T2-weighted MR image and corresponds to a lacuna. The images also show a well-delineated right posterior cortical watershed infarct. There is a mild surrounding gliosis and ipsilateral dilatation of the occipital horn of the lateral ventricle

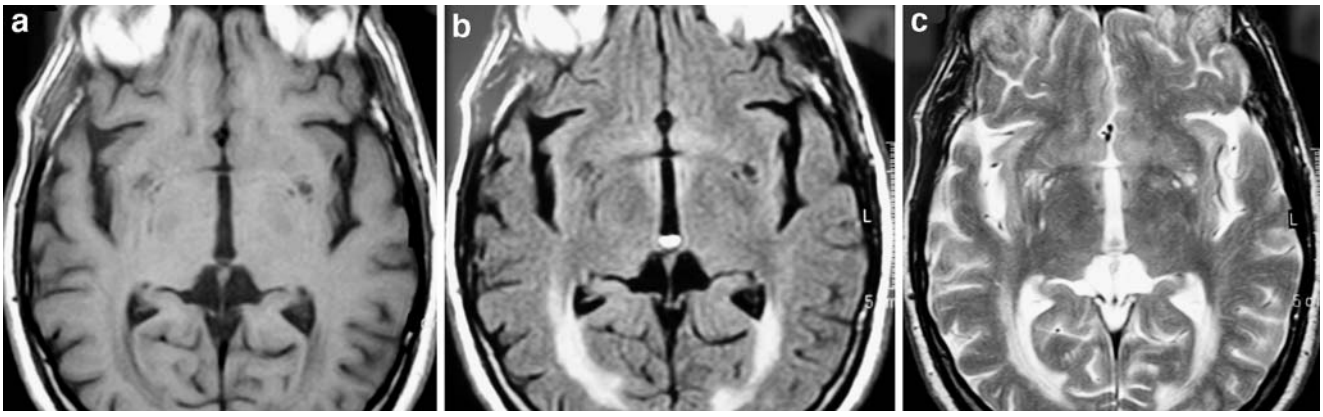

Fig. 25 Normal perivascular spaces in a 67-year-old patient with dementia. Axial **a** T1-weighted, **b** FLAIR, and **c** T2-weighted MR images show normal Virchow-Robin spaces located at the level of the anterior commissure. The slight asymmetry between the two sides is a normal finding

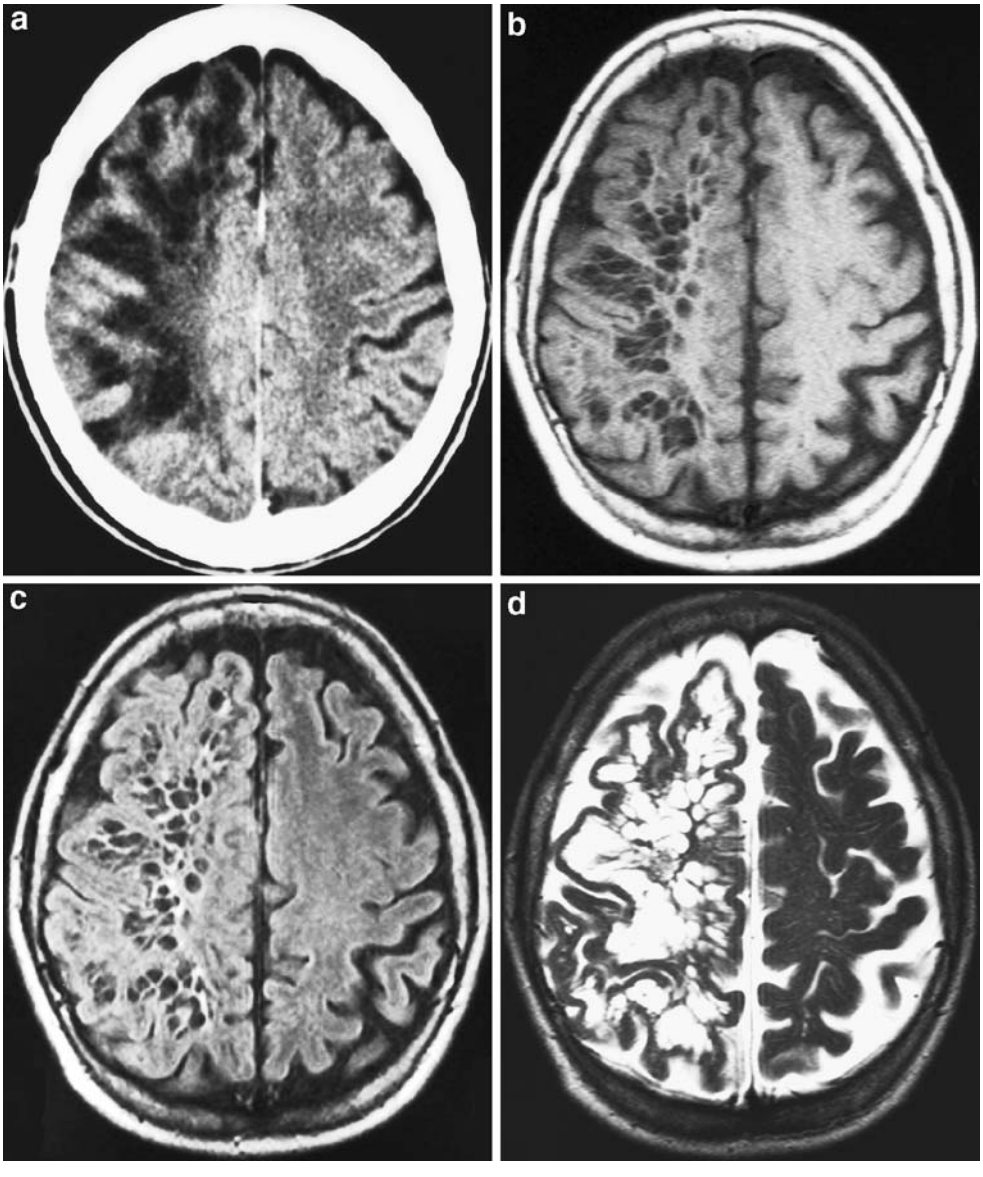

Fig. 26 Widespread dilatation of Virchow-Robin spaces in a 67-year-old man with cognitive deterioration. **a** Axial CT scan shows large hypodensity in the right centrum semiovale without mass effect, thought to be related to chronic large infarct. Axial **b** T1-weighted, **c** FLAIR and **d** spin-echo T2-weighted MR images disclose cyst-like structures with a radial pattern related to evident widened Virchow-Robin spaces

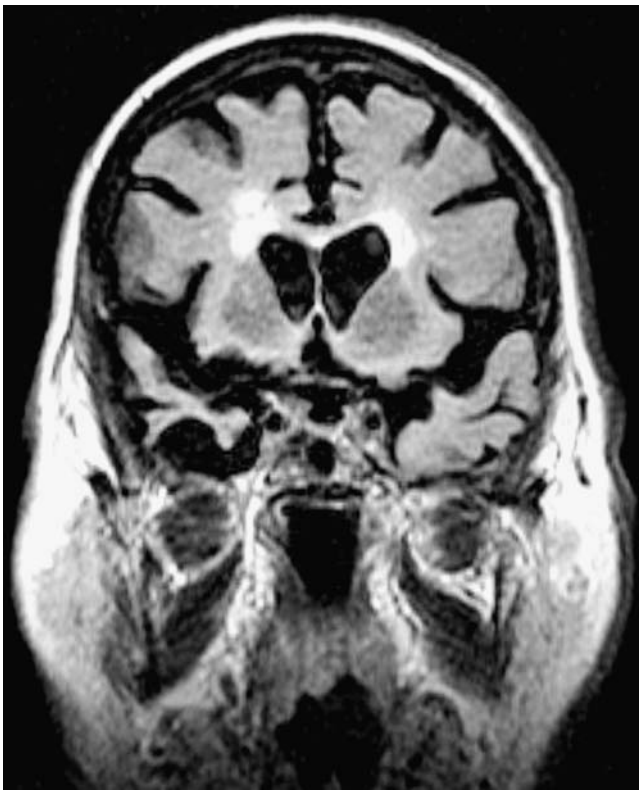

Fig. 27 Temporal atrophy in an 81-year-old woman with dementia. Coronal FLAIR MR image shows a global cerebral atrophy with a striking atrophy of the right temporal lobe. The corpus callosum is also atrophic and periventricular white matter hyperintensities are also seen

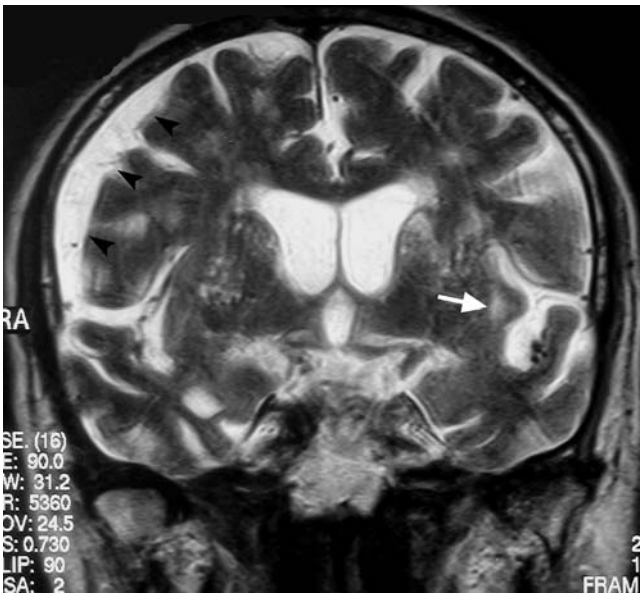

Fig. 29 Subdural hematoma, état criblé, brain atrophy and white matter changes in an 83-year-old man with rapid deterioration of his mental functions. Coronal spin-echo T2-weighted MR image shows a right hyperintense subdural fluid collection corresponding to chronic subdural hematoma (*arrowheads*). The cerebral structures are slightly shifted to the left side. There is also a mild widening of the perivascular spaces in the basal ganglia, enlargement of lateral ventricles, periventricular hyperintensities, and left preinsular white matter hyperintensity (*arrow*)

disease. The extent and location of the injuries differ considerably from patient to patient. Locations of the lesions, volume of destroyed tissue, multiplicity and bilateral occurrence are most important parameters underlying the clinical manifestations of VaD. A small injury in a strategic location can be of particular importance in some patients. Neuroimaging can also lead to a better understanding of symptoms and may help guide therapy. Finally, these criteria also require a temporal correlation between time of stroke onset and dementia. Early diagnosis of VaD is needed, and early administration of disease-stabilizing or disease-modifying therapies is highly recommended.

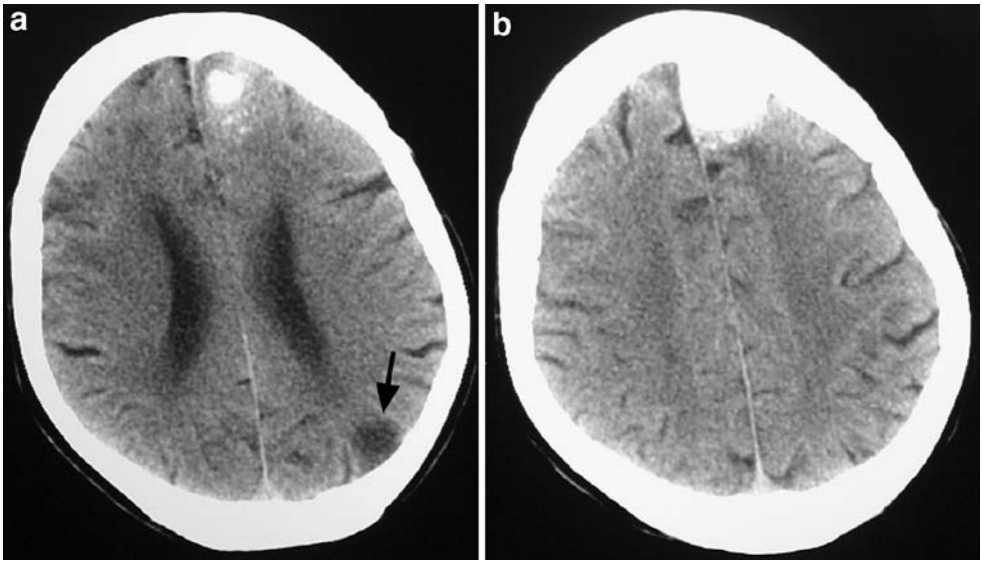

Fig. 28 Meningioma and watershed infarct in a 67-year-old woman with slowing down of mental functions. **a**, **b** Axial unenhanced CT scans show a large left frontal calcified lesion without surrounding edema corresponding to meningioma. There is also a left posterior cortical watershed infarct (*arrow*)

References

1. Erkinjuntti T (2002) Diagnosis and management of vascular cognitive impairment and dementia. J Neural Transm Suppl 63:91–109
2. Roman GC, Erkinjuntti T, Wallin A, Pantoni L, Chui HC (2002) Subcortical ischaemic vascular dementia. Lancet Neurol 1:426–436
3. Erkinjuntti T (1994) Clinical criteria for vascular dementia: the NINDS-AIREN criteria. Dementia 5:189–192
4. Roman GC, Tatemichi TK, Erkinjuntti T, Cummings JL, Masdeu JC, Garcia JH, Amaducci L, Orgogozo JM, Brun A, Hofman A, et al (1993) Vascular dementia: diagnostic criteria for research studies. Report of the NINDS-AIREN International Workshop. Neurology 43:250–260
5. Gold G, Giannakopoulos P, Montes-Paixao Junior C, Herrmann FR, Mulligan R, Michel JP, Bouras C (1997) Sensitivity and specificity of newly proposed clinical criteria for possible vascular dementia. Neurology 49:690–694
6. Lopez OL, Larumbe MR, Becker JT, Rezek D, Rosen J, Klunk W, DeKosky ST (1994) Reliability of NINDS-AIREN clinical criteria for the diagnosis of vascular dementia. Neurology 44:1240–1245
7. Pohjasvaara T, Mantyla R, Ylikoski R, Kaste M, Erkinjuntti T (2000) Comparison of different clinical criteria (DSM-III, ADDTC, ICD-10, NINDS-AIREN, DSM-IV) for the diagnosis of vascular dementia. National Institute of Neurological Disorders and Stroke-Association Internationale pour la Recherche et l'Enseignement en Neurosciences. Stroke 31:2952–2957
8. Roman GC (2003) Vascular dementia: distinguishing characteristics, treatment, and prevention. J Am Geriatr Soc 51:S296–S304
9. Erkinjuntti T, Rockwood K (2003) Vascular dementia. Semin Clin Neuropsychiatry 8:37–45
10. Erkinjuntti T (1997) Vascular dementia: challenge of clinical diagnosis. Int Psychogeriatr 9:51–58; discussion 77–83
11. Small GW (2002) The role of neuroimaging in the diagnosis of vascular dementia. Acta Neurol Scand Suppl 178:10–14
12. Kalaria RN, Ballard C (1999) Overlap between pathology of Alzheimer disease and vascular dementia. Alzheimer Dis Assoc Disord 13:S115–S123
13. Knopman DS, DeKosky ST, Cummings JL, Chui H, Corey-Bloom J, Relkin N, Small GW, Miller B, Stevens JC (2001) Practice parameter: diagnosis of dementia (an evidence-based review). Report of the Quality Standards Subcommittee of the American Academy of Neurology. Neurology 56:1143–1153
14. Nyenhuis DL, Gorelick PB (1998) Vascular dementia: a contemporary review of epidemiology, diagnosis, prevention, and treatment. J Am Geriatr Soc 46:1437–1448
15. Gold G, Giannakopoulos P, Seux AL, Zekry D, Michel JP (1998) Vascular dementia. Differential diagnosis and therapeutic issues. Ann Med Interne (Paris) 149:202–208
16. Leys D, Pasquier F (1999) Arterial hypertension and cognitive decline. Rev Neurol (Paris) 155:743–748
17. Leys D, Pasquier F, Parnetti L (1998) Epidemiology of vascular dementia. Haemostasis 28:134–150
18. Leys D, Erkinjuntti T, Desmond DW, Schmidt R, Englund E, Pasquier F, Parnetti L, Ghika J, Kalaria RN, Chabriat H, Scheltens P, Bogousslavsky J (1999) Vascular dementia: the role of cerebral infarcts. Alzheimer Dis Assoc Disord 13:S38–S48
19. Pasquier F, Henon H, Leys D (1999) Risk factors and mechanisms of post-stroke dementia. Rev Neurol (Paris) 155:749–753
20. Meyer JS, Muramatsu K, Mortel KF, Obara K, Shirai T (1995) Prospective CT confirms differences between vascular and Alzheimer's dementia. Stroke 26:735–742
21. Desmond DW, Moroney JT, Sano M, Stern Y (2002) Incidence of dementia after ischemic stroke: results of a longitudinal study. Stroke 33:2254–2260
22. Erkinjuntti T (2002) Cognitive decline and treatment options for patients with vascular dementia. Acta Neurol Scand Suppl 178:15–18
23. Erkinjuntti T (2002) Treatment options: the latest evidence with galantamine (Reminyl). J Neurol Sci 203–204:125–130
24. Erkinjuntti T, Kurz A, Gauthier S, Bullock R, Lilienfeld S, Damaraju CV (2002) Efficacy of galantamine in probable vascular dementia and Alzheimer's disease combined with cerebrovascular disease: a randomised trial. Lancet 359:1283–1290
25. Scheltens P, Fox N, Barkhof F, De Carli C (2002) Structural magnetic resonance imaging in the practical assessment of dementia: beyond exclusion. Lancet Neurol 1:13–21
26. Roman GC (2002) Vascular dementia revisited: diagnosis, pathogenesis, treatment, and prevention. Med Clin North Am 86:477–499
27. van Straaten EC, Scheltens P, Knol DL, van Buchem MA, van Dijk EJ, Hofman PA, Karas G, Kjartansson O, de Leeuw FE, Prins ND, Schmidt R, Visser MC, Weinstein HC, Barkhof F (2003) Operational definitions for the NINDS-AIREN criteria for vascular dementia: an interobserver study. Stroke 34:1907–1912
28. Pohjasvaara T, Mantyla R, Salonen O, Aronen HJ, Ylikoski R, Hietanen M, Kaste M, Erkinjuntti T (2000) How complex interactions of ischemic brain infarcts, white matter lesions, and atrophy relate to poststroke dementia. Arch Neurol 57:1295–1300
29. Mantyla R, Pohjasvaara T, Vataja R, Salonen O, Aronen HJ, Standertskjold-Nordenstam CG, Kaste M, Erkinjuntti T (2000) MRI pontine hyperintensity after supratentorial ischemic stroke relates to poor clinical outcome. Stroke 31:695–700
30. Dettmers C, Solymosi L, Hartmann A, Buermann J, Hagendorff A (1997) Confirmation of CT criteria to distinguish pathophysiologic subtypes of cerebral infarction. AJNR Am J Neuroradiol 18:335–342
31. Derdeyn CP, Khosla A, Videen TO, Fritsch SM, Carpenter DL, Grubb RL Jr, Powers WJ (2001) Severe hemodynamic impairment and border zone–region infarction. Radiology 220:195–201
32. Wong EH, Pullicino PM, Benedict R (2001) Deep cerebral infarcts extending to the subinsular region. Stroke 32:2272–2277
33. Gass A, Oster M, Cohen S, Daffertshofer M, Schwartz A, Hennerici MG (1998) Assessment of T2- and T1-weighted MRI brain lesion load in patients with subcortical vascular encephalopathy. Neuroradiology 40:503–506
34. Krapf H, Widder B, Skalej M (1998) Small rosarylike infarctions in the centrum ovale suggest hemodynamic failure. AJNR Am J Neuroradiol 19:1479–1484
35. Schmidt R, Schmidt H, Fazekas F (2000) Vascular risk factors in dementia. J Neurol 247:81–87
36. Boone KB, Miller BL, Lesser IM, Mehringer CM, Hill-Gutierrez E, Goldberg MA, Berman NG (1992) Neuropsychological correlates of white-matter lesions in healthy elderly subjects. A threshold effect. Arch Neurol 49:549–554
37. Kertesz A, Black SE, Tokar G, Benke T, Carr T, Nicholson L (1988) Periventricular and subcortical hyperintensities on magnetic resonance imaging. 'Rims, caps, and unidentified bright objects'. Arch Neurol 45:404–408
38. Mantyla R, Aronen HJ, Salonen O, Korpelainen M, Peltonen T, Standertskjold-Nordenstam C, Erkinjuntti T (1999) The prevalence and distribution of white-matter changes on different MRI pulse sequences in a post-stroke cohort. Neuroradiology 41:657–665
39. de Groot JC, de Leeuw FE, Oudkerk M, Hofman A, Jolles J, Breteler MM (2001) Cerebral white matter lesions and subjective cognitive dysfunction: the Rotterdam Scan Study. Neurology 56:1539–1545
40. Pantoni L, Leys D, Fazekas F, Longstreth WT Jr, Inzitari D, Wallin A, Filippi M, Scheltens P, Erkinjuntti T, Hachinski V (1999) Role of white matter lesions in cognitive impairment of vascular origin. Alzheimer Dis Assoc Disord 13:S49–S54

41. Schmidt R, Fazekas F, Kapeller P, Schmidt H, Hartung HP (1999) MRI white matter hyperintensities: three-year follow-up of the Austrian Stroke Prevention Study. Neurology 53:132–139
42. Barber R, Scheltens P, Gholkar A, Ballard C, McKeith I, Ince P, Perry R, O'Brien J (1999) White matter lesions on magnetic resonance imaging in dementia with Lewy bodies, Alzheimer's disease, vascular dementia, and normal aging. J Neurol Neurosurg Psychiatry 67:66–72
43. Salonen O, Autti T, Raininko R, Ylikoski A, Erkinjuntti T (1997) MRI of the brain in neurologically healthy middle-aged and elderly individuals. Neuroradiology 39:537–545
44. Scheltens P, Barkhof F, Leys D, Pruvo JP, Nauta JJ, Vermersch P, Steinling M, Valk J (1993) A semiquantative rating scale for the assessment of signal hyperintensities on magnetic resonance imaging. J Neurol Sci 114:7–12
45. Leys D, Henon H, Pasquier F (1998) White matter changes and poststroke dementia. Dement Geriatr Cogn Disord 9 [Suppl 1]:25–29
46. Guttmann CR, Benson R, Warfield SK, Wei X, Anderson MC, Hall CB, Abu-Hasaballah K, Mugler JP 3rd, Wolfson L (2000) White matter abnormalities in mobility-impaired older persons. Neurology 54:1277–1283
47. Erkinjuntti T, Inzitari D, Pantoni L, Wallin A, Scheltens P, Rockwood K, Roman GC, Chui H, Desmond DW (2000) Research criteria for subcortical vascular dementia in clinical trials. J Neural Transm Suppl 59:23–30
48. Roman GC (1999) New insight into Binswanger disease. Arch Neurol 56:1061–1062
49. Longstreth WT Jr, Manolio TA, Arnold A, Burke GL, Bryan N, Jungreis CA, Enright PL, O'Leary D, Fried L (1996) Clinical correlates of white matter findings on cranial magnetic resonance imaging of 3301 elderly people. The Cardiovascular Health Study. Stroke 27:1274–1282
50. Scheltens P, Erkinjunti T, Leys D, Wahlund LO, Inzitari D, del Ser T, Pasquier F, Barkhof F, Mantyla R, Bowler J, Wallin A, Ghika J, Fazekas F, Pantoni L (1998) White matter changes on CT and MRI: an overview of visual rating scales. European Task Force on Age-Related White Matter Changes. Eur Neurol 39:80–89
51. Wahlund LO, Barkhof F, Fazekas F, Bronge L, Augustin M, Sjogren M, Wallin A, Ader H, Leys D, Pantoni L, Pasquier F, Erkinjuntti T, Scheltens P (2001) A new rating scale for age-related white matter changes applicable to MRI and CT. Stroke 32:1318–1322
52. Mantyla R, Erkinjuntti T, Salonen O, Aronen HJ, Peltonen T, Pohjasvaara T, Standertskjold-Nordenstam CG (1997) Variable agreement between visual rating scales for white matter hyperintensities on MRI. Comparison of 13 rating scales in a poststroke cohort. Stroke 28:1614–1623
53. Chawda SJ, De Lange RP, Hourihan MD, Halpin SF, St Clair D (2000) Diagnosing CADASIL using MRI: evidence from families with known mutations of Notch 3 gene. Neuroradiology 42:249–255
54. Auer DP, Putz B, Gossl C, Elbel G, Gasser T, Dichgans M (2001) Differential lesion patterns in CADASIL and sporadic subcortical arteriosclerotic encephalopathy: MR imaging study with statistical parametric group comparison. Radiology 218:443–451
55. Bots GT (1992) Neuropathological findings in cerebral B-protein amyloidosis. Differences and similarities in those cases presenting as a cerebral hemorrhage and those presenting as a dementia of the Alzheimer type. Clin Neurol Neurosurg [Suppl] 94 S52–S53
56. Weller RO, Preston SD (2001) The spectrum of vascular disease in dementia. From ischaemia to amyloid angiopathy. Adv Exp Med Biol 487:111–122
57. Good CD, Ng VW, Clifton A, Britton JA, Hart Y, Wilkins P (1998) Amyloid angiopathy causing widespread miliary haemorrhages within the brain evident on MRI. Neuroradiology 40:308–311
58. Hendricks HT, Franke CL, Theunissen PH (1990) Cerebral amyloid angiopathy: diagnosis by MRI and brain biopsy. Neurology 40:1308–1310
59. Longstreth WT Jr, Bernick C, Manolio TA, Bryan N, Jungreis CA, Price TR (1998) Lacunar infarcts defined by magnetic resonance imaging of 3660 elderly people: the Cardiovascular Health Study. Arch Neurol 55:1217–1225
60. Leys D, Pasquier F, Lucas C, Pruvo JP (1995) Magnetic resonance imaging in vascular dementia. J Mal Vasc 20:194–202
61. Van Der Werf YD, Weerts JG, Jolles J, Witter MP, Lindeboom J, Scheltens P (1999) Neuropsychological correlates of a right unilateral lacunar thalamic infarction. J Neurol Neurosurg Psychiatry 66:36–42
62. Van der Werf YD, Scheltens P, Lindeboom J, Witter MP, Uylings HB, Jolles J (2003) Deficits of memory, executive functioning and attention following infarction in the thalamus; a study of 22 cases with localised lesions. Neuropsychologia 41:1330–1344
63. Olsson Y, Brun A, Englund E (1996) Fundamental pathological lesions in vascular dementia, Acta Neurol Scand Suppl 168:31–38
64. Bastos Leite AJ, van Straaten EC, Scheltens P, Lycklama G, Barkhof F (2004) Thalamic lesions in vascular dementia: low sensitivity of fluid-attenuated inversion recovery (FLAIR) imaging. Stroke 35: 415–419
65. Vital C, Julien J (2000) Expanding lacunae causing triventricular hydrocephalus. J Neurosurg 93:155–156
66. Adachi M, Hosoya T, Haku T, Yamaguchi K (1998) Dilated Virchow-Robin spaces: MRI pathological study. Neuroradiology 40:27–31
67. Bokura H, Kobayashi S, Yamaguchi S (1998) Distinguishing silent lacunar infarction from enlarged Virchow-Robin spaces: a magnetic resonance imaging and pathological study. J Neurol 245:116–122
68. Pullicino PM, Miller LL, Alexandrov AV, Ostrow PT (1995) Infraputaminal 'lacunes'. Clinical and pathological correlations. Stroke 26:1598–1602
69. Song CJ, Kim JH, Kier EL, Bronen RA (2000) MR imaging and histologic features of subinsular bright spots on T2-weighted MR images: Virchow-Robin spaces of the extreme capsule and insular cortex. Radiology 214:671–677
70. Adachi M, Hosoya T, Haku T, Yamaguchi K (1998) Dilated Virchow-Robin spaces: MRI pathological study. Neuroradiology 40:27–31
71. Poirier J, Derouesne C (1998) Distinguishing lacunar infarcts from dilatations of the perivascular space. J Neurol 245:813–814
72. Vital C, Julien J (1997) Widespread dilatation of perivascular spaces: a leukoencephalopathy causing dementia. Neurology 48:1310–1313
73. Uggetti C, Egitto MG, Pichiecchio A, Sinforiani E, Bevilacqua MS, Cavallini A, Micieli G (2001) Subcortical dementia associated with striking enlargement of the Virchow-Robin spaces and transneural degeneration of the left mammillo-thalamic tract. Cerebrovasc Dis 12:287–290
74. Mascalchi M, Salvi F, Godano U, Nistri M, Taiuti R, Tosetti M, Villari N, Calbucci F (1999) Expanding lacunae causing triventricular hydrocephalus. Report of two cases. J Neurosurg 91:669–674
75. Frisoni GB, Scheltens P, Galluzzi S, Nobili FM, Fox NC, Robert PH, Soininen H, Wahlund LO, Waldemar G, Salmon E (2003) Neuroimaging tools to rate regional atrophy, subcortical cerebrovascular disease, and regional cerebral blood flow and metabolism: consensus paper of the EADC. J Neurol Neurosurg Psychiatry 74:1371–1381
76. Fein G, Di Sclafani V, Tanabe J, Cardenas V, Weiner MW, Jagust WJ, Reed BR, Norman D, Schuff N, Kusdra L, Greenfield T, Chui H (2000) Hippocampal and cortical atrophy predict dementia in subcortical ischemic vascular disease. Neurology 55:1626–1635

77. Thacker NA, Varma AR, Bathgate D, Stivaros S, Snowden JS, Neary D, Jackson A (2002) Dementing disorders: volumetric measurement of cerebrospinal fluid to distinguish normal from pathologic findings – feasibility study. Radiology 224:278–285
78. O'Brien JT, Paling S, Barber R, Williams ED, Ballard C, McKeith IG, Gholkar A, Crum WR, Rossor MN, Fox NC (2001) Progressive brain atrophy on serial MRI in dementia with Lewy bodies, AD, and vascular dementia. Neurology 56:1386–1388
79. Giubilei F, Bastianello S, Paolillo A, Gasperini C, Tisei P, Casini AR, Gragnani A, Bozzao L, Fieschi C (1997) Quantitative magnetic resonance analysis in vascular dementia. J Neurol 244:246–251
80. Yamauchi H, Fukuyama H, Shio H (2000) Corpus callosum atrophy in patients with leukoaraiosis may indicate global cognitive impairment. Stroke 31:1515–1520
81. Tohgi H, Yonezawa H, Takahashi S, Sato N, Kato E, Kudo M, Hatano K, Sasaki T (1998) Cerebral blood flow and oxygen metabolism in senile dementia of Alzheimer's type and vascular dementia with deep white matter changes. Neuroradiology 40:131–137
82. Waldman AD, Rai GS (2003) The relationship between cognitive impairment and in vivo metabolite ratios in patients with clinical Alzheimer's disease and vascular dementia: a proton magnetic resonance spectroscopy study. Neuroradiology 45:507–512
83. Orgogozo JM, Rigaud AS, Stoffler A, Mobius HJ, Forette F (2002) Efficacy and safety of memantine in patients with mild to moderate vascular dementia: a randomized, placebo-controlled trial (MMM 300). Stroke 33:1834–1839
84. Roman G (2001) Diagnosis of vascular dementia and Alzheimer's disease. Int J Clin Pract Suppl 120:9–13